2008

A Structural and Biochemical Analysis of the Drosophila Protein Period

Heather Anne King

A STRUCTURAL AND BIOCHEMICAL ANALYSIS OF THE *DROSOPHILA* PROTEIN PERIOD

A Thesis Presented to the Faculty of

The Rockefeller University

in Partial Fulfillment of the Requirements for

the degree of Doctor of Philosophy

by

Heather Anne King

June 2008

A STRUCTURAL AND BIOCHEMICAL ANALYSIS OF THE *DROSOPHILA* PROTEIN PERIOD

Heather Anne King, Ph.D.
The Rockefeller University 2008

Circadian clocks regulate changes in behavior and physiology that occur with a period of approximately 24 hours and are based on negative feedback loops. The molecular components of circadian clocks are conserved among animals, and a key element in all such clocks is the protein Period (PER), a circadian transcription inhibitor. The stable production, post-translational modification, and nuclear translocation of PER all contribute to the timing of the clock. This work describes the synthesis and purification of various *Drosophila* PER fragments for biochemical and crystallographic analysis. Several stable PER fragments are identified, including one crystallizable fragment. The structure of the crystallized fragment is provided, and the implications of a critical intermolecular PER-PER interaction are explored.

The crystallized region of PER includes the PAS (PER-ARNT-SIM) domain (230-512) as well as two subsequent helices (512-575). Unlike a previously published structure for a similar fragment [1], this structure shows a closed

PER homodimer that relies on a flexible hydrophobic interaction between the final helix of one molecule and the PAS domain of its partner. Biochemical and mutational analyses of the crystallized fragment confirm the robust yet dynamic quality of this interaction. A critical residue in the dimerization interaction, Valine 243 is positioned at the center of the hydrophobic interface. Previous research has established that a lengthened-period phenotype in flies is caused by a point mutation at this residue, which changes the valine to asparitc acid [2]. Further studies have shown that the long period of flies bearing this mutation (*per*^{Long} flies) results from a delay in the PER nuclear translocation [3]. Disruption of the hydrophobic molecular interface introduced by V243D suggests the delay in nuclear entry associated with *per*^{Long} may be related to a defect in the PER self-binding interaction demonstrated in the crystal structure. The proximity of the observed PER-PER binding interface to the proposed PER-TIM binding interfaces also introduces the possibility that PER self binding may affect on the PER-TIM interaction. This work concludes with a proposed model for how disrupting the observed PER-PER intermolecular interaction may delay nuclear entry.

ACKNOWLEDGEMENTS

I would first like to thank Dr. Michael Young for allowing me to pursue a biochemistry and structure project in his laboratory. I would also like to thank Dr. Brian Crane for inciting my interest in both circadian clocks and structural biology. I am grateful to my committee chair, Seth Darst, for his insightful comments and helpful advice. I thank Dr. Andre Hoelz for demonstrating a genuine love for and commitment to scientific research and for taking an interest in this project. I also thank Peter Stavropoulos and Dr. Ivo Melcák for their guidance in biochemical and crystallography techniques. Jonathan Stieglitz was an excellent student who set many crystal trays for me, including the tray that produced the first crystal, and participated in many of the chromatography experiments. Toby Lieber and Simon Kidd kindly assisted me in learning molecular biology protocols. Lino Saez taught me how to work in a biology laboratory and provided wise counsel on many occasions. I thank Dr. Daniel Seay for his thoughtful advice and discussions, Asha Sarma for her excellent work as a technician and her camaraderie, and other former and present members of

Young Lab, including Catharine Boothroyd, Pablo Meyer, Saul Kivimae, Herman Wijen, Karina De La Punta, Nicholas Stavropoulos, Christine Ponder, Alina Patke, Dragana Rogulja, Sheyum Syed, and Eva Papadimas. The Cornell-Rockefeller-Sloan Kettering Tri-Institutional Training Program in Chemical Biology, headed by Dr. Tim Ryan, made this research possible with financial support and by encouraging me to reconsider a graduate career in physical chemistry and to instead apply myself to solving biological problems. I would also like to thank my husband and sons, Brett, Gray and Henry, for supporting this venture along with my parents, Susan and Gary King, – especially my mother, who made the writing of this thesis possible.

TABLE OF CONTENTS

LIST OF FIGURES

LIST OF TABLES

LIST OF ABBREVIATIONS

SCN	supra chiasmatic nucleus
RNA	ribonucleic acid
DNA	deoxyribonucleic acid
bHLH	basic helix-loop-helix
PAS	Per-Arnt-Sim
CCID	CLK/CYC inhibition domain
CLD	cytoplasmic localization domain
PCR	Polymerase chain reaction
IPTG	isopropyl-beta-D-thiogalactopyranoside
EDTA	ethylene diamine tetra acetic acid
PEI	polyethylene amine
SDS	sodium dodecyl sulfate
PAGE	polyacrylamide gel electrophoresis
FPLC	fast protein liquid chromatography
PER	Period
FRQ	Frequency
WCC	White Collar Complex
WC1	White Collar 1
WC2	White Collar 2
VVD	Vivid
TIM	Timeless
DBT	Doubletime
CLK	Clock

CYC	Cycle
bHLH	basic helix-loop-helix
SGG	Shaggy
CK2	Casein Kinase 2
CRY	Cryptochrome
SLMB	Slimb
VRI	Vrille
PDP	Par Domain Protein
BMAL	Brain and muscle aryl hydrocarbon receptor nuclear translocator-like
RORA	RAR-related orphan receptor A
CK1	Casein Kinase 1
B-TRCP	Beta-transducin repeat containing protein
GSK-3	Glycogen synthetase kinase 3
PDF	Pigment dispersing factor
HERG	Human ether-a-go-go
LOV	Light-oxygen-voltage
PYP	Photoactive Yellow Protein

PART 1. INTRODUCTION

1.1 The Discovery of Circadian Clocks

De Mairan, an early circadian biologist

The term circadian comes from the Latin and means about ("circa") daily ("dian") and describes phenomena that occur with a rhythm of approximately 24 hours. Circadian behaviors in living organisms have been documented as far back as the 4th century BC when an Alexandrian scribe wrote about heliotropism, the daily leaf movements of certain plants [4]. In the 1700s, Jean de Mairan showed that heliotropes continue to move with a near 24-hour rhythm even in constant darkness at constant temperature. This work suggested an internal timing mechanism.

Circadian biology in the twentieth century

Two centuries later, scientists again began to study the phenomena of circadian behaviors. Maynard Johnson, like DeMairan, observed circadian

rhythms that continued in darkness [5]. He studied the locomotor activity of deer mice, which follows a circadian pattern. The period of these mice became slightly longer than 24 hours in constant conditions, which helped argue against unseen geophysical forces (which would have more exact 24-hour cycles) driving circadian behavior. Some scientists, however, continued to argue that external forces, rather than an endogenous mechanism, controlled biological timekeeping.

The first light entrainment studies

Erwin Bunning and Hans Kalmus helped to establish the endogenous nature of circadian rhythms and the possibility of a dedicated biological timekeeping system ("ein bioligische Uhr" or "a circadian clock"). In the 1930s, their observations of *Drosophila* eclosion (hatching from the pupal case) demonstrated that rhythms could be reset and entrained by light [4]. The phase of the circadian period followed the light/dark entrainment regimen imposed on flies in the laboratory and was not drawn back to real time by unseen gravitational or other geophysical force. Using light as a *zeitgeber*, or time-giver, Bunning and Kalmus could dictate the subjective time understood by the animal. These experiments laid the groundwork for

many key experiments later in the century. One flaw in their work was the proposal that circadian timing in *Drosophila*, unlike other organisms studied, was sensitive to temperature [6]. Although temperature sensitivity would argue against exogenous control by forces independent of local temperature, it would also distinguish the *Drosophila* circadian rhythm from the temperature-independent rhythms described in plants and birds [7]. Further, it made little sense that any advantageous system for timekeeping could be strongly susceptible to modest fluctuations in temperature.

Establishing general qualities of circadian clocks

Colin Pittendrigh, who also studied circadian behavior in flies, realized that temperature-sensitivity conflicted strongly with his notion of a useful internal biological clock. A temperature-sensitive mechanism would rule out his hunch that the sun-compass navigation of starlings, as described in Gustav Kramer's work, was dependent on a general circadian timekeeping mechanism [7]. Pittendrigh knew if unifying principals of circadian clocks were to emerge, temperature compensation in all clocks would be a prerequisite. He repeated the temperature shift experiments but recorded the effects of temperature shifts on *Drosophila* rhythms for several days. He

concluded that although the circadian period is significantly altered after a temperature shift, as Kalmus claimed, this initial response to temperature transition lasts only a few cycles before flies regain their original 24-hour rhythmicity [6]. Once this hurdle had been overcome, Pittendrigh and his colleague, Jurgen Aschoff, began a thorough analysis of formal circadian properties which led to his 1960 lecture at the Cold Spring Harbor Symposia on Qualitative Biology, "Circadian rhythms and the circadian organization of living systems" [8]. Qualities common to all clocks were described, including persistence in the absence of environmental input, entrainability by zeitgebers such as light, and temperature independence. This lecture helped unite circadian biologists in a common goal – defining a novel biological system designed for timekeeping and used to choreograph a variety of behaviors and metabolic states.

Locating the clock

Pittendrigh also participated in the search for the physiological seat of the circadian clock, which he located in the optic lobe of cockroaches through ablation and transplantation studies [9]. Curt Richter performed similar studies in rats and defined the hypothalamus, more specifically the super

chiasmatic nucleus (SCN), as the mammalian location of the essential pacemaker [10]. Defining clock physiology helped to define its mechanism. The ablation and transplantation experiments that established the physiology of the clock were the first step toward dissecting the physical substance of the clock. Until then, the output of the clock and the theory of clocks were the focus of most research. Irving Zucker described the impact of circadian physiologists saying, "Richter succeeded in prying the lid off the circadian black box when he showed that unspecified lesions eliminated circadian activity and feeding rhythms" [5]. Physiologists acted as the forebears to geneticists and protein chemists by tinkering with certain parts of the clock, observing the results, and then selectively replacing (transplanting) these parts to restore function. Today this same type of breaking and fixing is the essence of work performed by not only circadian physiologists and geneticists, but also by biochemists and structural biologists.

Identifying circadian mutants

Our current understanding of the molecular mechanism underlying the clock has depended greatly on two organisms that are well characterized genetically and exhibit obvious circadian behaviors - *Drosophila*

melanogaster and *Neurospora crassa*. In 1971, Seymour Benzer and Ronald Konopka screened randomly mutagenized *Drosophila* and discovered strains of long-period, short-period, and arrhythmic flies [11]. Circadian rhythms in eclosion patterns and locomotor activity provided dependable, quantifiable data for identifying these mutants. A similar study was then undertaken using *Neurospora crassa*, producing a comparable period-altered circadian mutant [12]. *Neurospora crassa* has provided a useful model system for the study of circadian rhythms because conidation in these filamentous fungi occurs once per day according to the circadian rhythm of the organism. The length of filamentous growth between spore bands is directly proportional to time, providing a convenient assay of circadian period in this organism. No other systems appeared damaged or altered in the circadian mutants, suggesting the mutated genes were specific to timekeeping.

Cloning circadian genes

Although a single locus was identified as the cause of observed rhythm phenotypes both in *Drosophila* and in *Neurospora*, many years passed before the actual genes were identified, sequenced, and put to use in further defining the clock components. The *Drosophila* gene responsible for the

phenotypes observed by Benzer and Konopka, was the first to be defined [13, 14]. Once this key clock gene, named *period* (*per)*, could be cloned into expression constructs with inducible promoters, a host of new experiments became possible, many based on the rescue of rhythms in knockouts [15]. Recombinant expression of the Period made the production of PER antibody possible, allowing researchers to follow its abundance and localization [16]. The *Neurospora* gene frequency (frq) was also identified during this time, so that clocks from two very different species, flies and fungus, could be compared at the molecular level [17]. Although the clock components of these systems are not homologous, the clocks demonstrated a common basic mechanism; a continuous loop of transcription by a specific two-component circadian transcription factor followed by repression by a clock-specific negative feedback repressor [18]. Variations on this model are seen in the circadian clocks of bacteria, plants, and mammals as well as flies and fungus. Among metazoans, circadian components are homologous, The similarity between the insect and mammalian systems has facilitated the development of molecular models for both systems since the discovery of mammalian PER homologs in 1997 [19].

1.2 The physiology of the master clock

The molecular components of circadian clocks are expressed in many cells. Overt circadian rhythms, however, depend on synchrony among individual cellular clocks. In complex organisms, this synchrony is established by "master clock" cells (also called "pacemaker" cells), which set the phase in surrounding cells. In order to set the phase properly, master clocks utilize information about light level, temperature, and nutrient availability. Stimuli that have the power to entrain clocks are called *zeitgebers* or time-givers. The location of pacemaker cells often allows them to be uniquely or particularly susceptible to entrainment by certain zeitgebers. Since light is the primary zeitgeber, the master clock is positioned to receive light input. In mammals, master clock cells are located in the superchiasmatic nucleus (SCN) of the hypothalamus, where they receive light information from the retinohypothalamic tract. In *Drosophila*, the master clock is found in the ventral lateral neurons just behind the optic lobe. A "local clock," which obeys the master clock but also influences surrounding cells, is found in the liver of mammals, where it may sense and relay information about food intake. A local clock is also found in the Malphigean tubes of the *Drosophila* gut. Local clocks influence several individual organs, but their

function depends on the intact structure of the master clock [10]. Pacemaker cells align the phases of other cells by transmitting hormonal signals. Synchrony throughout the organism influences health and well being and depends on communication between master and local clocks.

1.3 The molecular clock

Circadian clocks are molecular networks based on negative feed back loops and have common elements in species from bacteria to plants to animals as depicted in Figure 1.1 [20]. Animal clocks depend on highly regulated circadian transcription factors that transcribe various output genes as well as clock genes [21, 22]. "Negative elements" are inhibitory complexes that are modified throughout the 24-hour cycle, first to prevent and then to facilitate inhibition of the "positive element," a transcription factor. The interplay between positive and negative elements of the clock creates an oscillator defined by rhythmic peaks and lulls of circadian transcription. Previously, the timing of the clock was understood to depend on the gradual formation and accumulation of stable inhibitory complexes. Recent investigations suggest a more complex model, wherein a critical event pushes the cycle forward. This event acts as a rate limiting step to determine the period of the

clock, suggesting an "interval timer" model rather than an hourglass [23]. The timing of such a critical event would depend on a series of modifications to the inhibitory element and/or the transcription factor. Further defining the positive and negative elements of circadian clocks and the modifications involved in such critical events will greatly enhance our understanding of biological timekeeping.

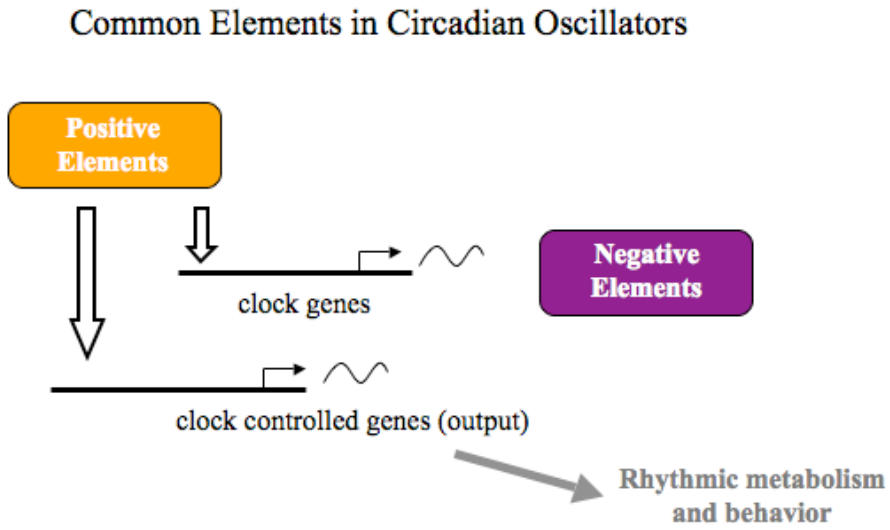

Figure 1.1. The basic components of a circadian clock, adapted from [18].

1.4 Conservation among clocks

Since the identification of the first circadian gene, *per*, in *Drosophila*, clock components have been described in *Neurospora*, Arabidopsis, Cyanobacteria, and Zebrafish as well as in mammals [20, 24-28]. The core clock genes are conserved among metazoans, and new clock and clock-related genes continue to be discovered, especially with the help of microarray analyses which have revealed genes whose expression levels vary according to a 24-hour cycle. The basic feedback mechanism of the clocks for *Neurospora*, *Drosophila*, and Mammals are described below. The *Drosophila* and mammalian systems are comprised of homologous proteins, while the *Neurospora* clocks consists of interesting counterparts from a system that appears to be independently evolved [29].

1.5 The *Neurospora* clock

The primary negative element in the *Neurospora* clock is the protein Frequency (FRQ) and the primary positive element is the White Collar Complex (WCC), comprised of two PAS proteins: White Collar 1 (WC1) and White Collar 2 (WC2) (see Figure 1.2a). The WCC transcribes a host of clock-controlled genes (ccgs), which influence circadian changes in

metabolism and reproduction. FRQ inhibits WCC activity in the morning hours with the help of the FRQ RNA helicase (FRH) [30]. Later in the day, FRQ promotes the accumulation of stable, inactive WCC complexes. In the evening, FRQ is degraded through the ubiquitin ligase FWD-1 and WCC activity is restored. The light-sensitive PAS protein Vivid (VVD) tunes the cycle by disrupting WCC complex formation in the early morning and promoting the degradation of frq mRNA in the evening [31]. In this manner, VVD tunes the clock by making the onset of circadian transcription more gradual in the morning and supports the elimination of FRQ in the evening. Many of the interactions of clock components in *Neurospora* depend on regulated phosphorylation and dephosphorylation, a common theme among circadian clocks. A schematic depicting the element of the *Neurospora* clock is provided in Figure 1.2a.

1.6 The *Drosophila* clock

The major negative elements of the *Drosophila* clock are PER and its binding partner, Timeless (TIM) (see Figure 1.2b). PER and TIM are two components of an inhibitory complex that also contains several kinases, including the PER-bound kinase Double-time (DBT), and may also include

other unknown components. The complex is gradually assembled in the cytoplasm throughout the day and in the evening undergoes changes that lead to the release of PER from TIM and the subsequent nuclear entry of PER, DBT, and TIM [23]. Inside the nucleus, PER/TIM inhibits circadian transcription. PER can also dissociate from TIM and inhibit transcription on its own [32]. Dissociation from TIM makes PER a more potent inhibitor but leads to PER phosphorylation and degradation in the nucleus as it does in the cytoplasm. The major positive element of the *Drosophila* clock is the transcription factor inhibited by PER/TIM and PER. It is a heterodimer of the proteins Clock (CLK) and Cycle (CYC), members of the basic helix-loop-helix (bHLH) PAS superfamily. CLK/CYC binds DNA E-box promoters that regulate the transcription of *per*, *tim*, and other clock-associated output genes [33].

Other clock components bolster and tune the basic auto inhibition loop described above. The kinase Double-time (DBT), which is part of the inhibitory complex, phosphorylates PER and targets it for degradation when TIM is not present [34-36]. Casein Kinase 2 (CK2) also phosphorylates PER to promote nuclear entry [37-39]. The GSK-3 homolog Shaggy (SGG)

has been shown to phosphorylate both TIM and CRY to regulate the clock [40]. Light input to the clock is mediated by Cryptochrome (CRY), which targets TIM for proteasomal degradation through the ubiquitin ligase Jetlag. When CRY destroys TIM, PER is phosphorylated by DBT and degraded with the help of the ubiquitin ligase, Slimb (SLMB), an F-box WD40-repeat protein that delivers phosphorylated PER to the proteasome [41, 42]. These components are listed in Table 1.1.

A secondary feedback loop compliments the primary loop shown above by controlling levels of CLK, the limiting factor in CLK/CYC formation and circadian transcription [43-45]. This loop depends on the genes *vrille* and *Pdp1,* which, like *per* and *tim*, are transcribed by CLK/CYC. These genes produce an inhibitor (VRI) and a promoter (PDP) of *Clk* expression. VRI accumulates first and inhibits *Clk* transcription. The resulting drop in CLK occurs when nuclear PER and TIM are high, further suppressing circadian transcription. As VRI levels taper off, PDP accumulates and reinstates *Clk* expression. This secondary loop sets up the next inhibition phase of the circadian cycle, since CLK/CYC inhibition by PER/TIM is compounded by a reduction in CLK levels due to VRI. In the phase after that, renewal of

CLK/CYC transcription is bolstered by a boost in CLK levels due to PDP. The secondary loop, therefore, supports and tunes the primary loop by aligning the peak in CLK concentration relative to the peak in CLK activity. A schematic depicting the elements of the *Drosophila* clock is provided in Figure 1.2b.

Interestingly, it has been shown that different sets of pacemaker cells in *Drosophila* with differential responses to light alternate in dictating the overall rhythm [42]. Evening cells, or E-cells, regulate circadian activity in light/dark conditions while morning cells (M-cells) drive the clock during the constant darkness of free-run. The molecular basis of the difference between E and M cells appears to involve changes in the interaction between CRY and TIM based on modifications by SGG.

Table 1.1: Components of the *Drosophila* circadian clock

Gene	Protein	Role	Interacts With	Known domains
clock (Clk)	CLK	Transcription factor, together with CYC transcribes clock and output genes	CYC, PER, E boxes	bHLH, PAS
cycle (cyc)	CYC	Transcription factor, together with CLK transcribes clock genes and output genes	CLK, PER, E boxes	bHLH, PAS
period (per)	PER	Transcription inhibitor	TIM, DBT, CLK/CYC, CRY, SLMB	PAS, Per C, Per S, NLS (2), CLD (2)
timeless (tim)	TIM	Transcription inhibitor	PER, CRY, SGG, CK2, CLK/CYC *	NLS, CLD
double-time (dbt)	DBT	Kinase phosphorylates PER, targets PER for degradation	PER	Ser/Thr kinase
slimb (slmb)	SLMB	A ubiquitin ligase, brings PER to proteasome	PER	F-box, WD40
jetlag (jet)	JET	A ubiquitin ligase, brings TIM to proteasome	TIM	F-box
cryptochrome (cry)	CRY	Intercepts light and causes TIM degradation	TIM, light (via flavin), PER	Photolyase, PAS
shaggy (sgg)	SGG	phosphorylates TIM, facilitates nuclear entry	TIM	Ser/Thr kinase

Casein kinase 2 (ck2)	CK2	phosphorylates TIM, facilitates nuclear entry	TIM	Ser/Thr (Tyr) kinase
vrille (vri)	VRILLE	inhibits *Clk* transcription, promotes *pdf* transcription	*Clk* promoter	bZIP
par domain protein-1 (Pdp-1)	PDP	promotes *Clk* transcription	*Clk* promoter	bZIP (PAR subfamily)

**TIM slightly inhibits CLK/CYC [46]*

1.7 The Mammalian clock

The primary negative elements of the mammalian clock are the *Drosophila* PER homologs mPER1, mPER2, and mPER3, which bind each other as well as the CRY homologs mCRY1 and mCRY2 (see Figure 1.2c). Although mCRY has sequence homology to *Drosophila* CRY, it behaves more like *Drosophila* TIM by binding, stabilizing, and promoting the nuclear entry of the mPERs. A TIM sequence homolog exists in mammals, but does not appear to play a substantial role in the circadian clock [47]. As in the fly clock, the positive element of the mammalian clock consists of two bHLH PAS proteins that form a transcription heterodimer. The mammalian sequence homolog of CLK is not the limiting factor in the pair. Rather, the

CYC homolog BMAL1 is limiting and cycles. Neuronal PAS domain protein 2 (NPAS2) can also bind BMAL1 to transcribe circadian genes. As in the *Drosophila* clock, levels of the limiting transcription factor (BMAL1) are controlled by a secondary loop [48]. This regulatory loop depends on *bmal1* inhibition by Rev-erbα to diminish the level of BMAL1 around the same time PER/CYC diminishes its activity. RORa then promotes *bmal1* transcription so that peak BMAL1 abundance coincides with peak circadian transcription. Kinases homologous to *Drosophila* DBT and SGG also exist in the mammalian clock. Like DBT, mammalian CK1 phosphorylates the mPER proteins and targets them for proteasomal degradation via the SLMB homolog β-TRCP [49, 50]. The SGG homolog GSK-3 phosphorylates the mammalian PER/CRY inhibitory complex to promote nuclear entry and may also affect the secondary loop of the clock through its ability to phosphorylate and stabilize the *Bmal1* inhibitor Rev-erbα [51] [[52].

Figure 1.2. Detailed molecular models of the *Neurospora*, *Drosophila*, and mammalian circadian clocks as depicted in [53] .

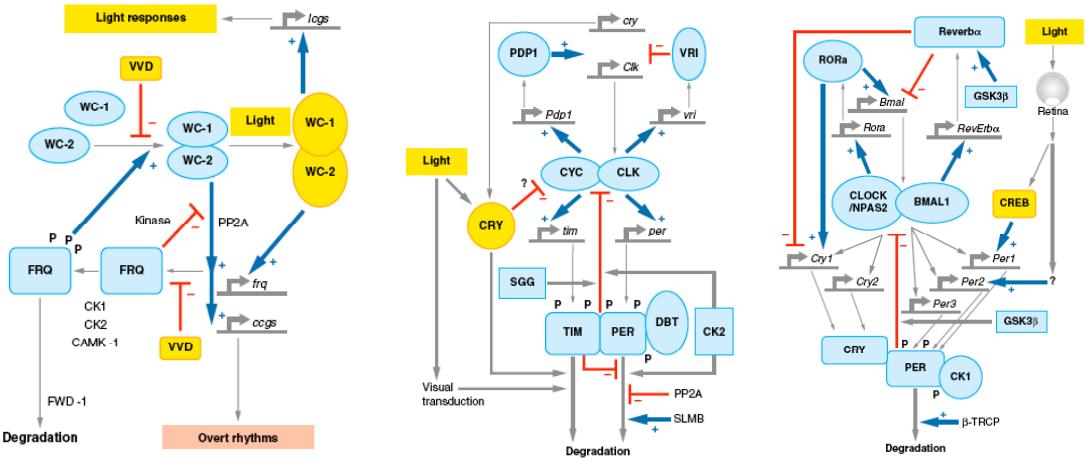

A. Neurospora B. Drosophila C. Mammalian

1.8 Human health and the clock

Circadian clocks have evolved because they allow organisms to predict daily changes in light and temperature based on the earth's rotation. They confer a further advantage by creating what Pittendrigh calls "temporal programming" within complex organisms wherein, "the predictable timing

of one cellular event determine(s) the optimum time for another" [7]. Disrupting normal clock function by crossing time zones or working a night shift not only prevents the body from anticipating meals, rest, or work demands but also upsets the temporal order among biological systems. Clocks affect DNA repair and mitosis. Clocks that are constantly disturbed by unpredictable circadian regimens (such as rotating shift work) or defective components (caused by mutations in clock genes) can lead to cancer [54] [55]. Bipolar disorder, schizophrenia, and seasonal affective disorder (SAD) have also been linked to the clock [56-58].

The importance of circadian rhythms for overall health continues to be supported by the literature and will make structural information about clock proteins increasingly relevant in the development of therapeutic targets for a range of medical conditions. Not only could targeted therapeutics help to repair compromised clock function, they could also be used to control global transcription of clock-controlled genes and prompt broad changes in physiological state.

The role of PER in the circadian clock

The 24 hour cycle of the clock can be viewed in terms of the transcription, translation, cytoplasmic accumulation, nuclear entry, inhibitory action, and subsequent breakdown of PER.

Transcription of *per* by CLK/CYC

In the early morning hours, the CLK/CYC transcription factor transcribes *per*, *tim*, the secondary loop genes *vri* and *Pdp1*, and various circadian controlled genes (ccgs) that govern circadian changes in behavior and physiology. After a significant delay (6 hours), *per* is translated, though the mechanism of translational regulation is unknown [59].

Formation of the PER-DBT-TIM (PDT) cytoplasmic complex

Once PER is produced, it rapidly forms a cytoplasmic complex with TIM and DBT that also includes the kinases CK2 and SGG. The availability of TIM determines the stability of PER, because when TIM is not present DBT phosphorylates PER to mark it for proteasomal degradation (via the F-box protein SLMB). DBT phosphorylation also plays a role in PER nuclear entry [60]. CK2 binds and phosphorylates PER to promote nuclear entry.

The GSK3 homolog Shaggy (SGG) binds and phosphorylates TIM to promote nuclear entry. The cytoplasmic complex may include other unidentified components. Its stochiometry and composition are unknown and may change throughout the day. This complex holds PER in the cytoplasm for many hours, contributing to the feedback delay that is essential for the 24-hour period of the clock.

Nuclear entry

Nuclear Entry of PER depends on several unknown factors that lead up to some critical event that involves the release of cytoplasmic PER and TIM into the nucleus. It has recently been discovered that the separation of PER and TIM is one aspect of this release [23]. A pattern of phosphorylation events involving DBT, CK2, and SGG has been shown to contribute to nuclear entry and may play a key role in the transformation of the cytoplasmic complex and the release of PER-DBT and TIM into the nucleus [39, 61]. One unexplained aspect of nuclear entry is the formation of concentrated bundles of fluorescently-labeled PER and TIM in S2 insect cell culture prior to entry, which appear as bright spots, or “punctae” and may reflect the sequestering of PER-DBT-TIM (PDT) complexes in subcellular

organelles, possibly endosomes, as one step of the nuclear entry process [23]. Entry into and exit from these locations would then be aspects of the interval timer mechanism, and mutations that delay nuclear entry could be viewed in terms of interfering with these events. Since PDT accumulate gradually into punctae and disperse rapidly immediately before nuclear entry, release from these punctae would coincide with the separation of PER from TIM that occurs during nuclear entry, which may be a critical aspect of the interval timer. A specific importin may carry PER and TIM to the nuclear pore complex, as is the case for the mammalian clock protein mCRY2 [62, 63].

Inhibition of CLK/CYC by PER

Inside the nucleus, a PDT complex forms again, though some PER remains free from TIM. Although both free and complexed PER are able to inhibit CLK/CYC, free PER does so more effectively. Free PER is susceptible to phosphorylation by DBT (and degradation), so that the release of PER from TIM, which occurs rapidly when light leads to TIM degradation, both encourages CLK/CYC inhibition and ends it. PER reaches its low point in the early hours, and circadian transcription by CLK/CYC begins a new

cycle. Repression of CLK/CYC depends on a region in the C-terminus of the protein referred to as the CLK/CYC inhibition domain (CCID) [64]. This region may act as a scaffold between CLK and the PER-bound kinase DBT or another kinase [65]. This mechanism of inhibition has been shown in the mammalian and in the *Neurospora* clock [66, 67]. It was initially speculated that PER might interfere with CLK/CYC transcription by binding one protein or the other through its PAS (Per-Arnt-Sim) domains in order to separate the two, but this was proved false [33]. Therefore, the function of the PER PAS domains remains unclear.

Figure 1.3. A basic schematic of the 24 hour PER cycle. The CLK/CYC transcription factor is shown in orange and yellow. PER is shown in purple and TIM is shown in blue.

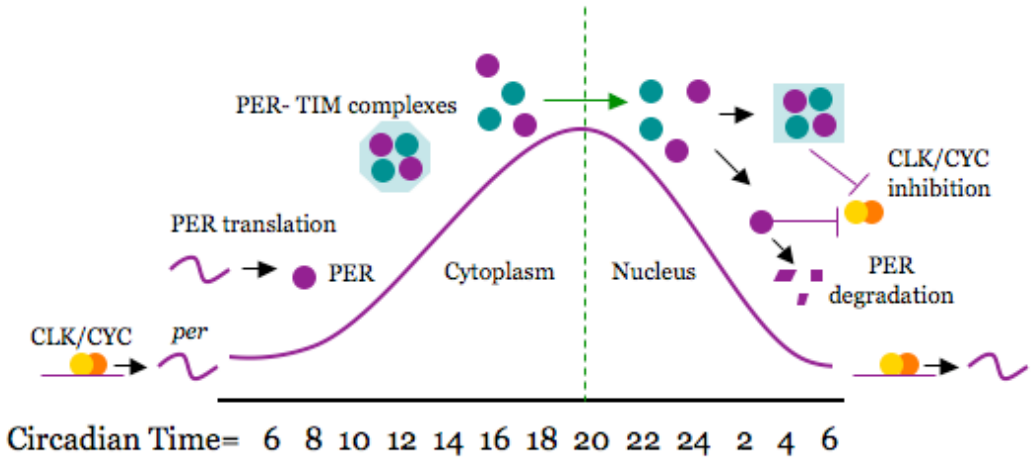

1.10 The PER protein

The PER PAS domains are found in the N-terminal half of the protein and between residues 240 and 512 (of 1224). These are the only regions of known structural homology, however, many other regions of PER have been characterized by their functionality. Residues responsible for binding other proteins or nuclear/cytoplasmic localization have been identified as well as residues that are phosphorylated by DBT and CK2. These are summarized on the function domain map in Figure 1.4, as are point mutations whose circadian phenotypes have been well characterized.

Figure 1.4. A Functional Map of the PER Protein

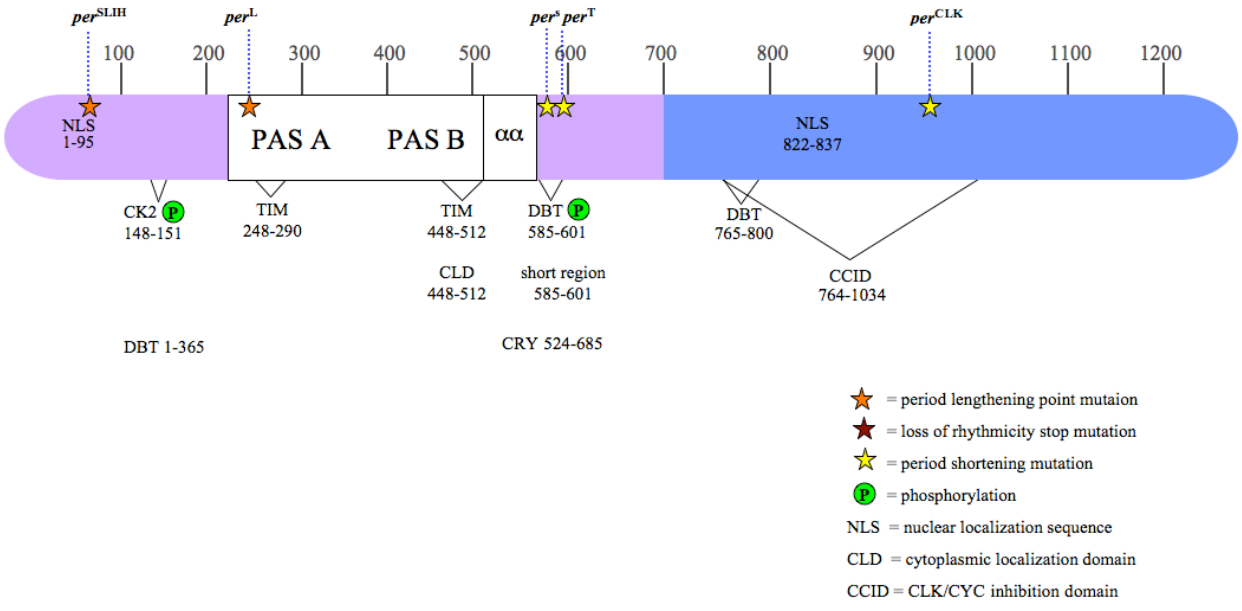

A more extensive list of PER features, such as binding regions, residues involved in point mutations, or residues that undergo regulated phosphorylation is provided in Table 1.2. Some features can be categorized according to what step of the PER cycle they affect. Some mutations or deletions affect several steps, so that the overall effect on rhythm must be dissected to properly interpret the behavioral change.

Table 1.2: PER features

Feature	Location	Involved with
Nuclear localization sequence	1- 95	Nuclear entry
SLIH mutant, (long rhythms, shorter with heat)	S45Y	Temperature compensation
Interaction with DBT	1- 365	Phosphorylation, Degradation
CK2 phosphorylation facilitates nuclear entry	149-151	Nuclear entry
Pas A domain	240-293	TIM binding (TIM 507-578)
Long mutant	V243D	Nuclear entry, Temperature compensation
Pas B domain	365-454	Unknown
Cytoplasmic localization domain (CLD)	448-512	Localization, TIM binding (TIM 715-914)

"Short" domain, regulated phosphorylation affects stability	585-600	Phosphorylation, Degradation
Short mutant	S589N	Nuclear Stability
Interaction with CRY	524-685	Stability following light pulse, Interaction with TIM
PER DBT (1-292) binding domain	765-800	DBT binding, Phosphorylation
dCLK:CYC inhibition domain	764-1034	Inhibition of CLK/CYC
Second NLS	822-837	Nuclear Entry
Clk mutant	A969V	Stability

PAS domains within PER

The PAS A and B domains of PER (shown in white in Figure 4 and listed in Table 2) follow the canonical PAS fold, which consists of a five-strand beta sheet sitting beneath a cluster of 4-5 alpha helices. The typical fold and nomenclature used to describe PAS domains are shown in Figure 1.5.

Figure 1.5. The Typical PAS Fold and Nomenclature as seen in the Human Ether-a-go-go related gene (HERG) protein [68].

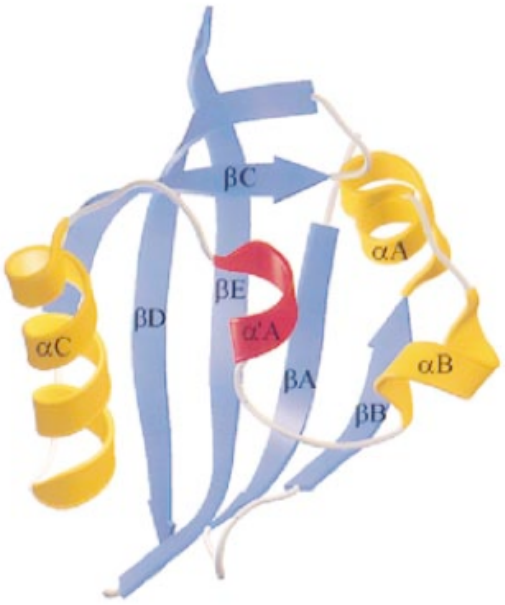

PAS stands for PER as well as ARNT, the aryl hydrocarbon receptor nuclear translocator protein (ARNT), and SIM, the *Drosophila* Single-minded protein. The PAS domain was initially defined as a 270 amino acid region containing a pair of highly conserved spans termed PAS A and PAS B. Later, when unpaired and multiple PAS repeats were discovered, the PAS definition was modified to describe single amino acid sequences with highly conserved N-termini [69, 70]. Since then, PAS domains have been found

throughout species from bacteria to mammals, and are predominantly located within cytosolic sensory proteins [69]. PAS domains fall into two broad categories, those that transmit information about light, oxygen levels, and voltage (also called LOV domains), and those that acts as protein-protein binding interfaces.

Structural data about PAS domains come from crystallized proteins, including the photoactive yellow protein (PYP) [71, 72], the N-terminal of a human potassium channel (HERG) [68], the FixL bacterial oxygen sensor [73, 74], and the LOV2 photoreceptor in plants [75]. These structures demonstrate a common α/β fold, however, the activity and specificity of each PAS domain is regulated by flanking domains and or co-factors [76]. Each structure shows a single PAS domain, and all except HERG include cofactors.

PAS domains and circadian clocks

PAS domains are found in the PER, CLK, and CYC *Drosophila* clock proteins as well as in their mammalian homologues. Table 3 lists PAS proteins involved in the *Drosophila* clock and in the human clock.

Table 1.3: PAS proteins involved in *Drosophila* and Mammalian Clocks

Organism	**Gene**	**Protein**	**PAS Interacts With**
Drosophila	*Period (per)*	PER	TIM, CLK/CYC,
Drosophila	*clock (Clk)*	CLK	CYC, PER,
Drosophila	*cycle (cyc)*	CYC	CLK, PER,
Human	*Period1 (per1)*	hPER1	CRY1&2, PER1-3 CLK/BMAL, CLK/NPAS2
Human	*Period (per2)*	hPER2	CRY1&2, PER1-3
Human	*Period (per3)*	hPER3	CRY1&2, PER1-3
Human	*brain and muscle aryl hydrocarbon receptor nuclear translocator-like 1 (bmal-1)*	BMAL1	CLK
Human	*(nPAS2)*	NPAS2	CLK
Human	*clock (Clk)*	CLK	BMAL1, NPAS2

PAS domains are also found in the circadian clock proteins of Cyanobacteria, Arabidopsis, and *Neurospora*. In *Drosophila* clocks, PAS

domains are thought to mediate protein-protein binding between PER and TIM and are not known to bind co-factors. In mammalian clocks, PAS domains are also known to mediate protein-proteins interactions. Additionally, the mammalian transcription factor NPAS2 binds a heme cofactor, and a murine PER (mPER2) may also bind heme [77, 78].

The PAS domains of the mammalian PERs

The mammalian PER homologues mPER2, and mPER3 contain tandem PAS domains with strong homology to the *Drosophila* PER PAS region. Elimination of the mPER2 PAS B domain in *mPer2*^{BrdmI} mutants (Δ348-434) leads to shortened rhythms in light/dark (LD) entrainment and arrhythmicity in constant darkness, suggesting the importance of the PAS domains in clock function [79] . Homodimerization and heterodimerization are known to occur in mammalian PERs, and likely occur via PAS-PAS interactions [80]. The N-terminal half of the mPER3 protein, which contains the PAS region and no other known protein interaction domains, is sufficient for heterodimerization with mPER1 and mPER2. Heterodimerization of mPERs regulates nuclear entry [81]. Binding between mPER3, which contains a nuclear localization sequence (NLS), and either mPER1 or mPER2 is shown

to facilitate nuclear entry in cell culture. In a separate study, nuclear mPER1 formed heterodimers with co-expressed mPER2 and became cytoplasmic. The PAS region of mPER3, which contains an NLS, is responsible for holding this protein in the cytoplasm. When the PAS domain is deleted, mPER3 localizes to the nucleus.

The PAS domains of PER

Although the discovery of PAS structural homology in PER was hailed "a landmark in the molecular map of circadian clocks," the role of the PER PAS domains is not yet known [82]. PER does not appear to inhibit CLK/CYC through PAS-PAS interactions that separate original heterodimer, as was originally suspected [33]. Furthermore, the PAS domains of PER are not part of the region determined by deletion analysis to be critical for inhibiting CLK/CYC [64]. Rather the PER PAS domains are required for binding TIM, which has no PAS sequence homology [83]. A hydrophobic residue in the PER PAS A domain (Valine 243) is mutated in per^{Long}, which exhibits delayed nuclear entry, suggesting this domain may be involved in nuclear entry, either directly or through an effect on the PER-TIM interaction. Interestingly, the PER-TIM interaction appears to be

strengthened rather than diminished in *per*^{Long}. [84] The cytoplasmic localization domain (CLD) of PER is also located in the PAS region. It is the beta sheet of the PER PAS B domain. Removing this domain holds otherwise nuclear PER in the cytoplasm. The beta sheets of PAS domains often mediate binding interactions, and deletion analysis shows that the PER PAS B beta sheet (residues 448-512) is necessary for an in vitro interaction between PER and TIM 715-914. A crystal structure of the PER PAS domain region of PER indicates PAS-PAS interactions could create PER oligomers, though the primary intermolecular interface is non-symmetrical which leads to the formation of octamers [1]. A new crystal structure, presented in this work, shows a symmetrical PAS-PAS interaction between PER molecules, leading to separate dimers. This structure demonstrates how the PAS domains can act as homodimeric interfaces between PER molecules, while leaving open areas identified as necessary for TIM binding. The homodimerization interface demonstrated in this structure uses an interesting mechanism that may allow multiple conformations and invite change or modification in interactions between PER and TIM or PER and the entire PER-TIM-DBT complex.

PART 2: MATERIALS AND METHODS

2.1 Molecular Biology

Period fragments were cloned from existing PER constructs for 1-700 and 1-1021 into pGEX6P3 using BamH1/Not1 cut sites to position the PER sequence downstream from the GST fusion protein. A stop codon was introduced into each fragment with the 3' oligomer. The oligomers used for polymerase chain reaction (PCR) to create the crystallized fragment are shown below.

at residue 229: BamH1 site
5' oligomer AGA GGA TCC CAG CGC GGG GAG CGG GTG AAG GAG
overhang **G Q R G E R V K E**

at residue 575:
5' CGG GCG GAT CTC AAG CTG GAG TAA GCG GCC GCA GAG
R A D L K L E stop
overhang
NotI site

3' oligomer CTC TGC GGC CGC TTA CTC CAG CTT GAG ATC CGC CCG

Following PCR and purification of PCR products, cutting with BamH1 and Not1 took place at 37˚C for 3-14 hours. Gel purified digested PCR products were ligated into cut plasmid at 16 ˚C overnight or at 21˚C for three hours. The ligation product was transformed into XLI cells by heat shock at 42˚C. Successfully transformed colonies were grown in 2 ml cultures to confluence, and vector DNA was extracted and purified using ion exchange minicolumns (Qiagen miniprep kit). Extracted DNA was cut by BamH1 and Not1 to verify incorporation of the PCR product. All other constructs were prepared similarly. Point mutations were introduced into pGEX6P3 using the QuikChange mutagenesis system (Stratagene). All clones were verified by sequencing.

2.2 Protein Expression and Purification

Vectors as described above were transformed into *E. coli* BL21 (pLysS), a chloamphenicol resistant E. coli strain that expresses T7 lysozyme to suppress basal expression of T7 RNA polymerase, thereby restricting expression of target protein prior to controlled induction with IPTG. T7 lysozyme also aided in lysis while the presence of chloramphenicol in stocks and cultures reduced the risk of contamination. As described in Figure 2.1,

transformed pLysS cells were grown to confluence overnight with shaking in LB with 50 micrograms/ml ampicillin or carbenicillin and 35 micrograms/ml chloramphenicol. Larger flasks of LB were inoculated with 0.2% v/v confluent culture and shaken at 37˚C to OD = 0.6 to 0.9 before induction with 0.5mM isopropyl-beta-D-thiogalactopyranoside (IPTG). After induction, the temperature was lowered to 20˚C, and cells were shaken for an additional 20-22 hours. Cells were collected by centrifugation at 5,000g for 10 minutes and resuspended in Buffer 1 or Buffer 2 (Buffer 1 = 50mM Tris (pH 7.5), 150mM NaCl, 3mM DTT, Buffer 2 = 50mM Tris (pH 7.5), 500mM NaCl, 3mM DTT).

EDTA-free protease inhibitor tablets (Roche) and recombinant DNAse (Roche) were added to the resuspension before freezing at -80˚C. Frozen cells were thawed with stirring at room temperature with 5% of a 10x detergent solution (Bug Buster). For preparations of fragments including residues 1-80, which strongly bind DNA (discussed in Part 3), 1 microliter/ 20ml resuspension RNAse cocktail with 1mg/ml RNAse A and 20,000U/ml RNAseT1 (Ambion) was added. The thawed lysate was passed through a syringe to shear DNA and incubated at 4˚C for 30 to 50 minutes until the

degradation of nucleic acid reduced the lysate viscosity sufficiently for centrifugation. Soluble protein was separated from solids by centrifugation at 20,000g for 45 minutes, and the resultant supernatant was incubated with 1-2 mcrl/ml 30% polyethylene amine (PEI) for 20 minutes on ice. Addition of PEI served to precipitate remaining nucleic acid from the soluble component. The supernatant was then respun at 12,000g to precipitate PEI-bound solids and filtered at 0.42 micron before adding rinsed, equilibrated glutathione sepharose beads (1 ml bead/Liter of culture). The bead and protein solution was nutated at 4˚C for 1 hour and the beads were spun down at 1,000g. The supernatant was then removed as "flow through" and the beads rinsed in batch (two 30ml rinses of Preparation Buffer per 1.5ml beads). Beads were then transferred to a column and rinsed with 10-12 column volumes more buffer, and Prescission protease was added (5-10 units per/ Liter culture) in a 1mM EDTA buffer. The column was left overnight at 4˚C. Eluted protein was concentrated using spin columns (10,000KD cutoff) and then run on Superdex 200 sizing column. Peak fractions were collected and analyzed for purity by PAGE. The most pure fractions were collected, concentrated, and exchanged to an appropriate buffer for crystallization trials (for the crystallized fragment, 20mM Hepes

(pH 7.7), 200mM NH_4HCO_3 was used). Hampton Crystal Screen and PEG screen were used as the initial screens for crystallization trials.

Figure 2.1. Standard purification protocol developed for purification of PER fragments expressed in E. coli.

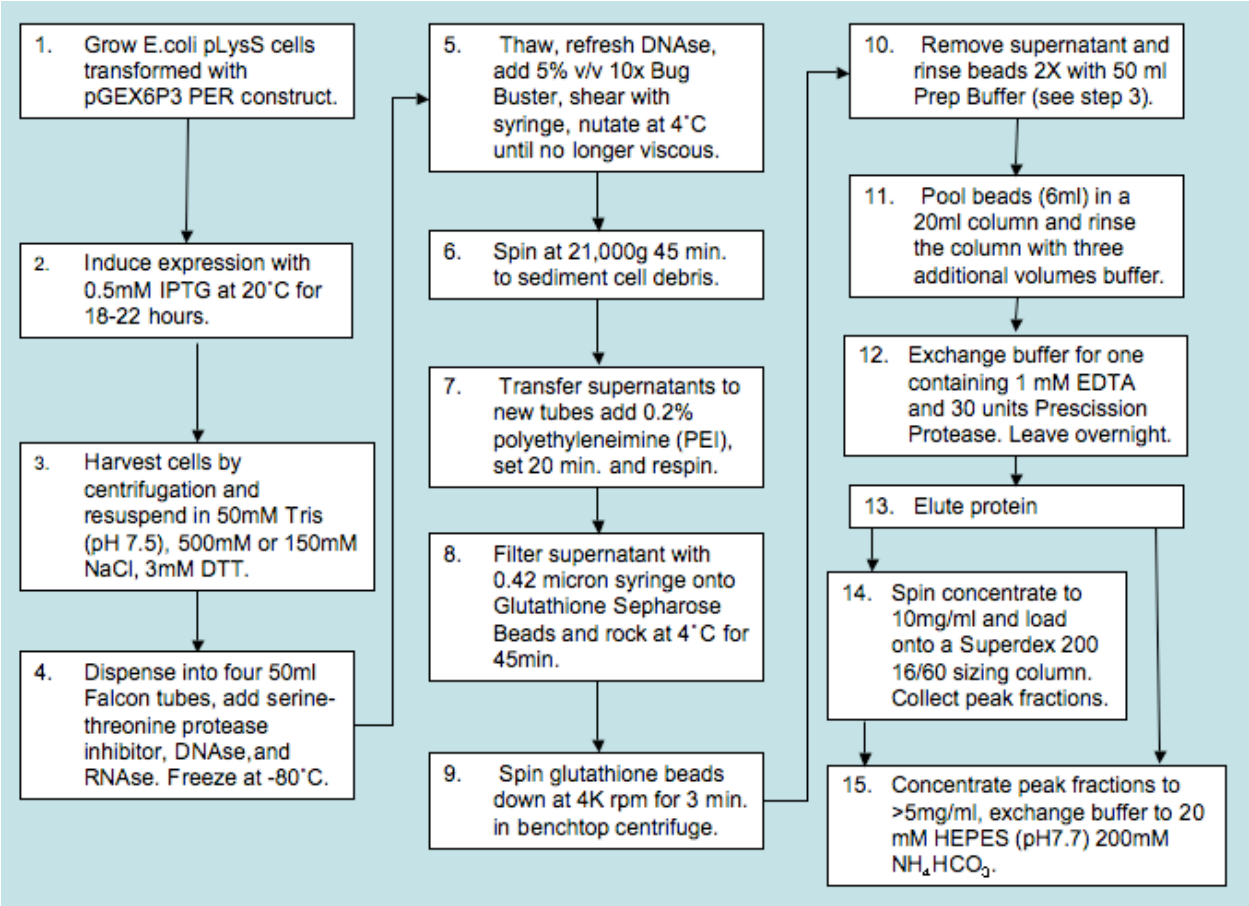

2.3 Protein analysis by SDS PAGE

Protein samples were separated according to their electrophoretic mobility using sodium dodecyl sulfate polyacrylamide gel electrophoresis (SDS PAGE). Gels were made with 6,8, and 4-12 (gradient)% acrylamide in bis/tris buffer and run at a constant voltage of 150-200mV.

2.4 Analytical Chromatography

Analytical gel filtration chromatography of affinity-purified PER fragments was performed using a SMART FPLC system with a 3.2/30 Superdex 200 column (Amersham Biosciences). Columns were pre-equilibrated with Buffer 1 or 2 (see above). Protein elution was monitored by measuring absorbance at 280 nm. In some cases, DNA elution was also measured by absorbance at 260. A calibration curve was generated by measuring the elution volumes of standard proteins of known molecular mass (Bio-Rad) shown below in Figure 2.2. Molecular masses of PER fragments were estimated based on elution volume and weight of the monomer as indicated by PAGE analysis of peak fractions.

Figure 2.2. A chromatogram showing the elution peaks of known molecular weight standards run on a Superdex 200 3.2/30 SMART column. Elution volumes as a percentage of column volumes are consistent with Superdex 200 16/60 and 26/60 columns.

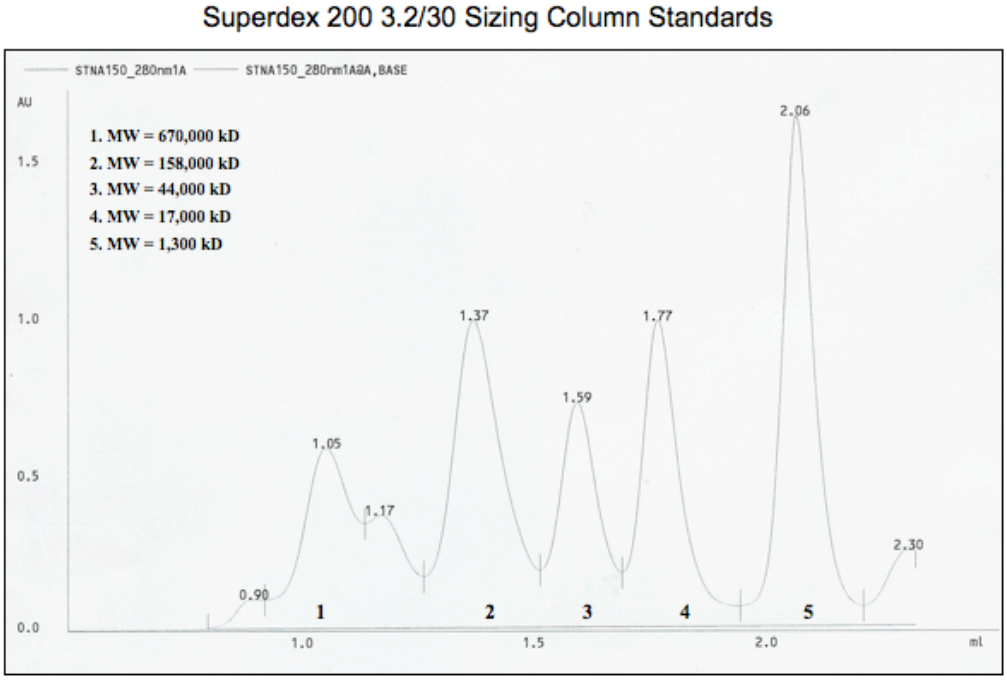

2.5 Crystallization

Crystals of PER 229-575 were grown at 20°C in hanging drop setups using a reservoir solution with 200mM lithium chloride, 20% PEG 3350 (15% PEG if seeded), 100mM Bicine (pH 9.0) and a protein solution with 5 mg/ml PER

229-575 in 20mM HEPES (pH 7.7), 200mM NH_4HCO_3, and 5mM DTT. For X-ray data collection at 100 K, crystals were transferred in several steps into a cryoprotecting solution containing 20% Glycerol (v/v), 200mM lithium chloride, 20% PEG 3350, and 100mM Bicine (pH 9.0) and shock frozen in propane. SeMet crystals were treated similarly.

2.6 Data Collection, Structure Determination, and Refinement

The crystals belong to space group P1 with cell constants a=60.4 Å, b=94.7 Å, c=141.0 Å and α=88.2°, β=89.6°, γ=89.9° and two molecules per asymmetric unit. Data to 2.85 Å resolution were collected from a single PER 229-575 crystal at 100 K using the BL8.2.1 beamline at ALS. The data set was processed with HKL2000. Molecular replacement with 1WA9 (residues 236-540) was used to calculate the phases. The 2.85 Å map was obtained after iterative rounds of model building into 2Fo - Fc and Fo - Fc maps and refinement using bulk solvent correction, positional, torsion angle simulated annealing, and grouped B factor refinement protocols of CNS. The model consists of 2,579 amino acids and 12 water molecules. Some residues in the loop regions are not seen in the electron density due to conformational disorder. Figures were generated using PyMOL.

Table 2.1. X-Ray Data Collection and Refinement Statistics

Data collection	
Synchrotron	ALS
Beamline	BL8.2.1
Space group	P1
Cell dimensions	
a, *b*, *c* (Å)	a=60.4, b=94.7, c=141.0
α, β, γ (°)	α=88.2°, β=89.6°, γ=89.9°
Wavelength (Å)	1.00000
Resolution (Å)	20.0-2.85
R_{sym} (%)	8.1 (63.0)
$\langle I / I \sigma \rangle$	14.2 (2.0)
Completeness (%)	92.4 (89.7)
Redundancy	3.3
Refinement	
Resolution (Å)	20.0 – 2.85
No. reflections	62,958
R_{work} / R_{free} (%)	25.7 / 28.7
No. atoms	22,356
R.m.s deviations	
Bond lengths (Å)	0.008
Bond angles (°)	1.4

PART 3: PURIFICATION OF STABLE PER FRAGMENTS

For crystallization trials and some chromatographic assays, several milligrams of highly pure protein are required. Such quantities of PER cannot be purified from *Drosophila* or from insect cell culture in a cost effective manner. In order to express large quantities of PER, fragments amenable to overexpression in E. coli must be determined. Fragments were selected to maximize the number of interesting functional domains or known mutations, many of which occur in the first 700 residues (see Figure 1.4).

The presence of domains of interest was balanced against the likelihood of successful crystallization. Sequence alignment (Blast, T-coffee) and secondary structure analysis (Predict Protein) were used to select N and C termini with strong alignment to homologous proteins and predicted structural elements. Constructs for expression of these fragments were prepared as described in Part 2, and small-scale induction trials helped to determine expression levels of various constructs. Solubility tests were then performed to show the partitioning of protein between the soluble fraction

and the insoluble cell pellet following lysis. Finally, small scale (50mL) affinity purification assays narrowed the pool of fragments to those that could be moved forward to large-scale preparations. Several stable fragments can be purified in large quantities, and extensive crystal screens of these fragments yielded crystals for the PER 229-575 fragment.

Figure 3.1. General method for selection of PER fragments to test for solubility

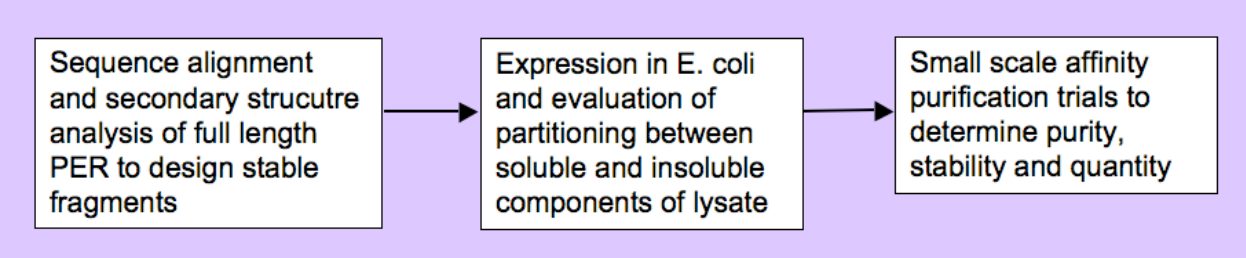

PER fragments fit for preparation of larger quantities (500mL-1L) are listed in Table 3.1. Of these, some strongly bind nucleic acid. Removal of N-terminal residues 1-87 eliminates nucleic acid binding. Truncation of the N-terminal 87 residues eliminates nucleic acid binding but leads to degradation of the C-terminus. These issues are described in Sections 3.1-3.2. One highly stable PER fragment neither binds DNA strongly nor degrades from

the C-terminus. This is PER 229-575, which can be crystallized using the method described in Section 3.3.

Table 3.1 PER fragments that are soluble and can be purified in large quantities from E. coli

PER Fragment	Nucleic Acid binding	Degradation	Crystallization screens	Successful Crystallization
1-848	Yes	Slight	Yes	No
1-700	Yes	Slight	Yes	No
1-629	Yes	Slight	No	No
1-575	Yes	Slight	Yes	No
87-700	No	Yes	Yes	No
87-848	No	Yes	No	No
147-692	No	Yes	Yes	No
147-573	No	No	Yes	No
170-700	No	Yes	Yes	No
205-692	No	Yes	Yes	No
229-848	No	Yes	Yes	No
229-628	No	Yes	Yes	No
229-575	No	No	Yes	Yes

PART 3.1 The N-terminus of PER binds nucleic acid

PER fragments that include residues 1-87 bind nucleic acid strongly, forming large soluble aggregates and hindering purification. RNAse treatment reduces the aggregation, as does increasing the salt concentration of the purification buffer. The resultant proteins are stable and pure but do not crystallize. Eliminating the N-terminal 87 residues of PER solves the problem of aggregation and the need for higher salt and RNAse treatment during purification but introduces a new problem - instability and proteolytic cleavage of the protein.

Data:

PER 1-700 forms a large, soluble aggregate and runs in the void of gel sizing columns, preventing further purification following affinity purification. The OD 260 reading of the chromatogram in Figure 3.1.1 indicates the presence of nucleic acid, and samples of PER 1-700 run on agarose gels are stained by ethidium bromide. Tandem equivalent purifications of 1-700, 147-573 and 147-692, show that although affinity purified PER 1-700 is strongly stained by ethidium bromide when run on a 1% agarose gel, similar preparations of

PER 147-573 and 147-692 are not. Residues 692-700 are not responsible for nucleic acid binding since PER 1-568 also binds nucleic acid (Figure 3.1.1). DNAse versus RNAse assays performed on affinity purified PER 1-700 and phenol extractions of purified PER 1-700 indicate that RNAse A/T1 cocktail breaks down the nucleic acid present, but DNAse does not (Figure 3.1.2). Stringent treatment of affinity purified PER 1-700 and PER 1-568 with RNAse eliminates aggregates, as seen in the change in the chromatograms of PER 1-700 and PER 1-568 following RNAse treatment (Figure 3.1.3); however, PER fragments that include the N-terminus and are purified in the manner do not crystallize after extensive trials.

Figure 3.1.1. Affinity purified PER 1-700 prepared in 150mM NaCl buffer runs as a large soluble aggregate on gel sizing columns. A. PER 1-700 runs in the void volume of a superdex 200 sizing column with strong OD 260 absorbance B. PAGE SDS analysis of eluted PER 1-700 C. Eluted PER 1-700 run on agarose gels shows strong ethidium bromide staining.

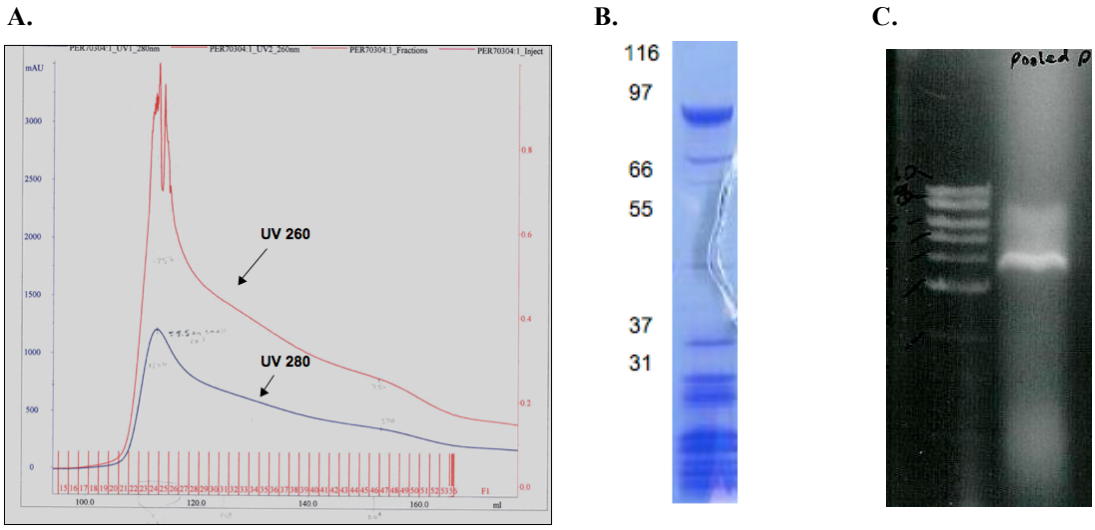

Figure 3.1.2. Affinity purified samples of 1-700, but not 147-573 or 147-692, are strongly stained by ethidium bromide. A. SDS PAGE gel with 1. Affinity purified PER 1-700, 2. Affinity purified PER 147-575, 3. Affinity purified PER 147-573. B. 1% Agarose gel with equivalent samples to A C. SDS PAGE showing four equivalent samples of 1-700 from A treated with 1. nothing, 2. Recombinant DNAse, 3. RNAse A + T cocktail, 4. Benzonase nuclease (a non-specific endonuclease) D. 1% Agarose gel with equivalent samples to C.

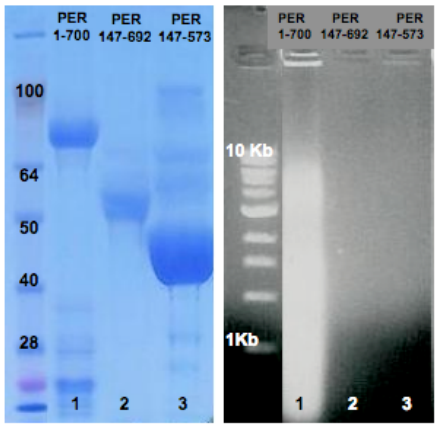

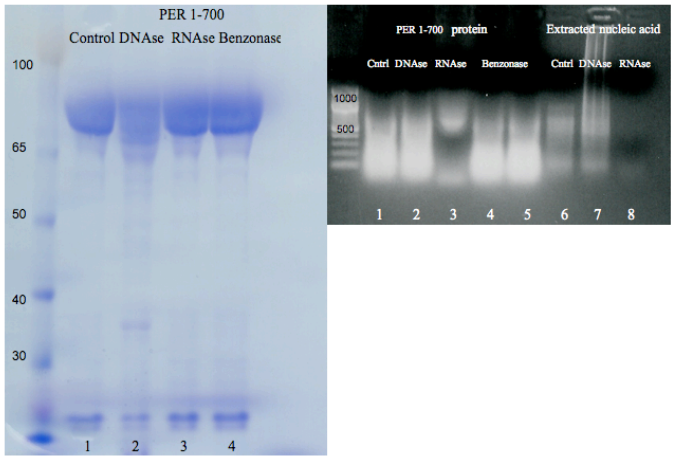

Figure 3.1.3. Treatment with RNAse cocktail (described in Part 2) breaks up the aggregates formed by PER 1-700 and by PER 1-575. A. As above, affinity purified Per 1-700 runs in the void volume of a Superdex 200 sizing column (>700,000kD). Following RNAse treatment, the aggregate is broken up, and the protein can be separated from impurities. B. Similarly, PER 1-568 behaves as an aggregate unless treated with RNAse. C. Using RNAse treatment along with a higher salt purification buffer (500mM versus 150mM NaCl), PER1-700, 1-575, and 1-848 can be prepared using the method described in Part 2 to fairly high purity.

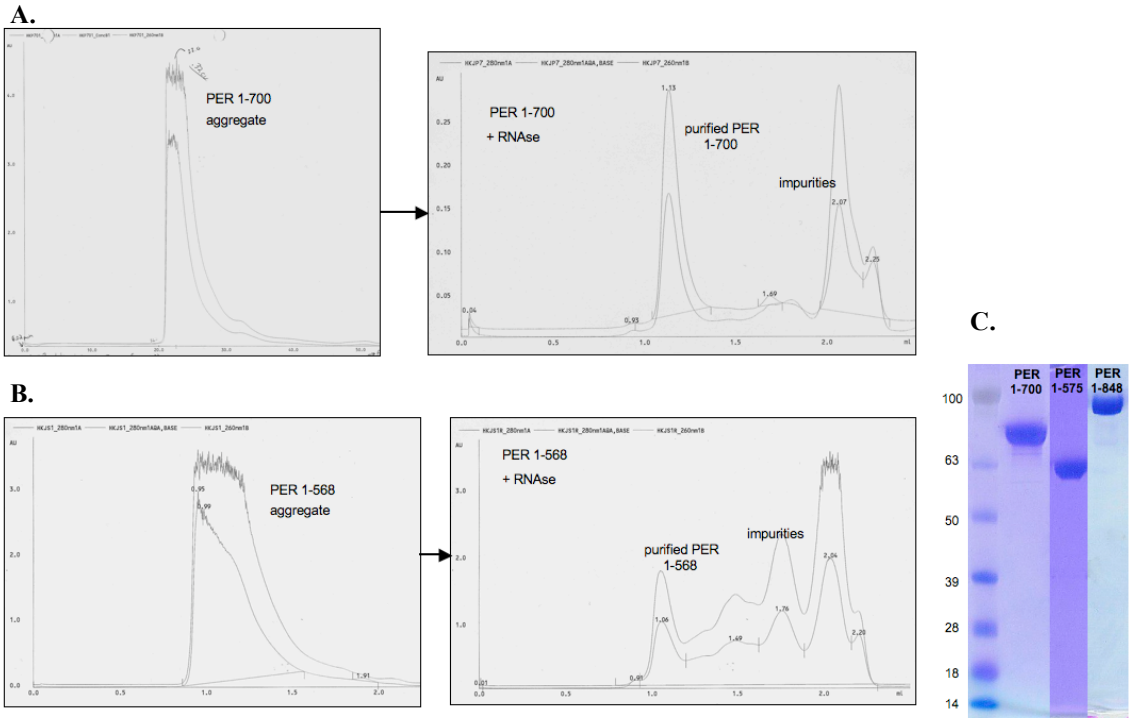

Conclusion

In order to purify PER fragments including residues 1-87, high salt and stringent RNAse treatment must be used. Even following such treatment, purified PER fragments that include the N-terminus do not crystallize after extensive screening. Failure to crystallize may or may not result from residual nucleic acid binding. To avoid nucleic acid binding, the N-terminus can be eliminated.

PART 3.2 Eliminating the N-terminus of PER destabilizes PER fragments that extend beyond residues at or around 570.

PER fragments that include residues 1-87 bind nucleic acid and form aggregates that hinder purification. Eliminating the N-terminal 87 residues of PER fragments does solve the problem of aggregation, but introduces a new problem - instability and proteolytic cleavage of the protein. PER fragments lacking the N-terminus, including 87-695, 87-848, 147-692, and 170-700 are unstable. Edman sequencing followed by mass spectrometry of the smallest degradation product of PER 170-700 indicates that this

fragment has an intact N-terminus beginning at 170 but a degraded C-terminus that ends at or around residue 570. This is consistent with the stability of the N-terminally truncated fragments 147-573 and 229-575, while similar proteins such as 147-692 and 229-848 are unstable and degrade to a finite size consistent with loss of the C-terminal end after residue 570.

Data:

Eliminating the N-terminus strongly reduces nucleic acid binding but causes protein instability. PER 87-695 does not form large soluble aggregate and The OD 260 trace of the chromatogram shown in Figure 3.2.1 does not indicate nucleic acid binding. The resultant protein is unstable, however, and degrades from 67 kD to a finite size around 50kD. The same type of degradation is seen in PER 87-848, but not 1-848. Proteolytic cleavage is also seen in PER 147-692 and 170-700.

Figure 3.2.1. N-terminally truncated PER does not aggregate but degrades. A. Per 87-695 can be purified by gel sizing chromatography without high salt or RNAse treatment B. Purified 87-695 is unstable and degrades. C. PER 87-848 is unstable compared to PER 1-848.

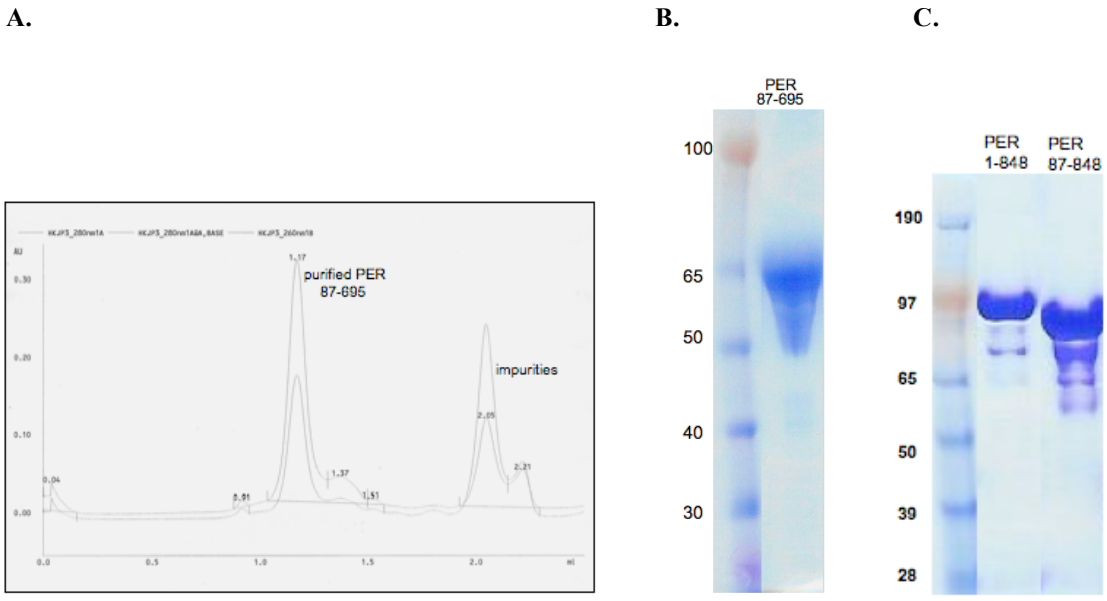

Figure 3.2.2. A. PER170-700 is less stable than PER 1-700 and shows similar patterns of degradation to 87-695 and 87-848. The smallest degradation band of PER 170-700 was submitted for Edman sequencing and mass spectrometry, and results indicate this band begins at residue 170 and ends at or around 570. B. 147-692 shows a similar pattern of degradation (arrow indicates protein). C. PER 147-573 does not show a similar degradation pattern.

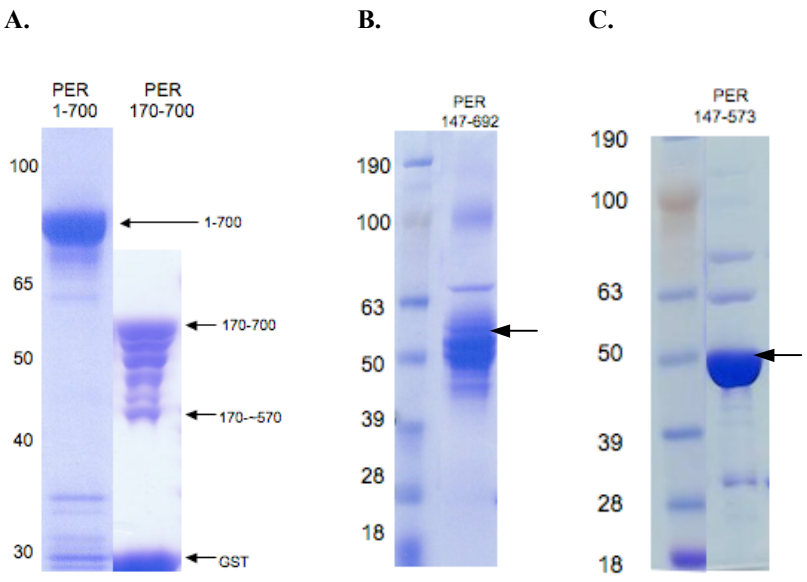

Conclusion

To avoid nucleic acid binding, the N-terminus of PER fragments can be eliminated, but this leads to degradation. The smallest product of this degradation in PER 170-700 begins at 170 and ends at or around 570. C-terminal degradation of N-terminally truncated fragments is consistent with the pattern of degradation seen in PER 87-695, 87-848, 147-692, and 170-700 as well as the stability of PER 147-573 and PER 229-575 (depicted in section 4). The following table describes PER fragments that appeared to be good candidates for crystallization following initial screens, problems in large-scale purification of these proteins and the one successfully crystallized fragment, PER 229-575. It is interesting to consider the possibility that the N-terminus of PER physically interacts with residues following 570 in the "short/mutable" region of PER (585-600). A variety of mutations in this region shorten the circadian rhythm *in vivo* [85] . This shortened rhythm comes from more rapid turnover of nuclear PER. If the N-terminus of PER interacts with the short/mutable region *in vivo*, mutations in the PER short region may destabilize PER by interrupting this interaction.

PART 3.3: Crystallization of PER 229-575

PER 229-575 produces stable, reproducible crystals with strong diffraction when prepared and crystallized as described in Part 2. A mutant version of PER 229-575 carrying the *per*^{Long} mutation (V243D) could not be crystallized. This and other versions of *per*^{Long}: V243D, V243R, and V243N, were far less soluble than wild type and ran as monomers or in a monomer-dimer equilibrium near monomer. The failure of these mutants to dimerize becomes apparent by looking at the position of V243 in the crystal structure. The effect of V243D on PER dimerization and its position in the crystals structure are discussed further in sections 4.6 and 6.

Data:

As shown in Figure 3.3.1, PER 229-575 can be purified cleanly and runs at approximately dimer molecular weight, though slightly smaller (some monomer-dimer equilibrium). The chromatogram in Figure 3.2.1 is from a column run in 150 mM salt, and PER 229-575 runs as a strict dimer only in 500mM NaCl. Purified PER 229-575 is quite clean, though after several

days a small band appears 2-3kD beneath the full-length fragment band, consistent with the loss of αF (residues 550-575). This underband does not appear when protein crystals are analyzed by PAGE. Crystals of PER 229-575 form overnight using the method described in section 2.

PER 229-575 V243D is far less soluble than the wild-type. The degradation band seen in wild-type protein is present from initial purification in V243D and far more prominent. The V243D protein runs in two peaks, one at a weight consistent with a monomer-dimer equilibrium and the other consistent with a strict monomer. Peak fractions indicate that the monomer peak consists of the slightly degraded protein. PER 229-575 V243D does not crystallize under conditions similar to those used for PER 229-575 nor does it crystallize using other general protein screens described in Part 2.

Figure 3.3.1. PER 229-575 purified by Gel Filtration: A. This fragment runs close to dimer size on gel filtration. Lines labeled "D" and "M" indicate peak volumes consistent with the dimeric and monomeric molecular weights. B. Lane 1 shows a peak fraction of 229-575 from a gel filtration column, Lane 2 shows purified PER 229-575 after several days at 4˚C.

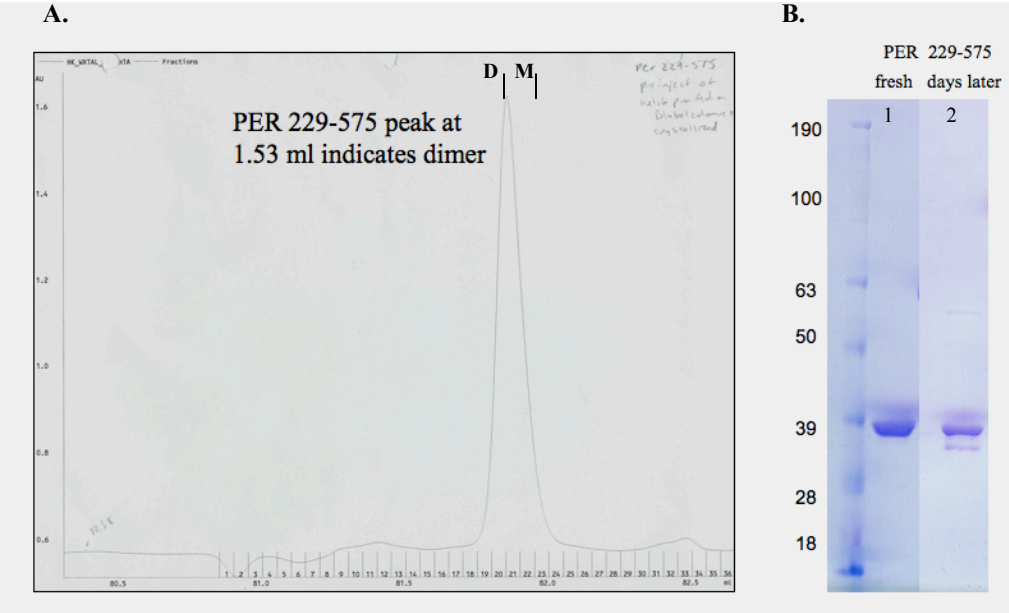

Figure 3.3.2. PER 229-575 crystallizes overnight at room temperature. A. Without seeding, PER forms large plates. B. With streak seeding, small single crystals grow, C. and D. Seeding with a stock solution produces larger single crystals.

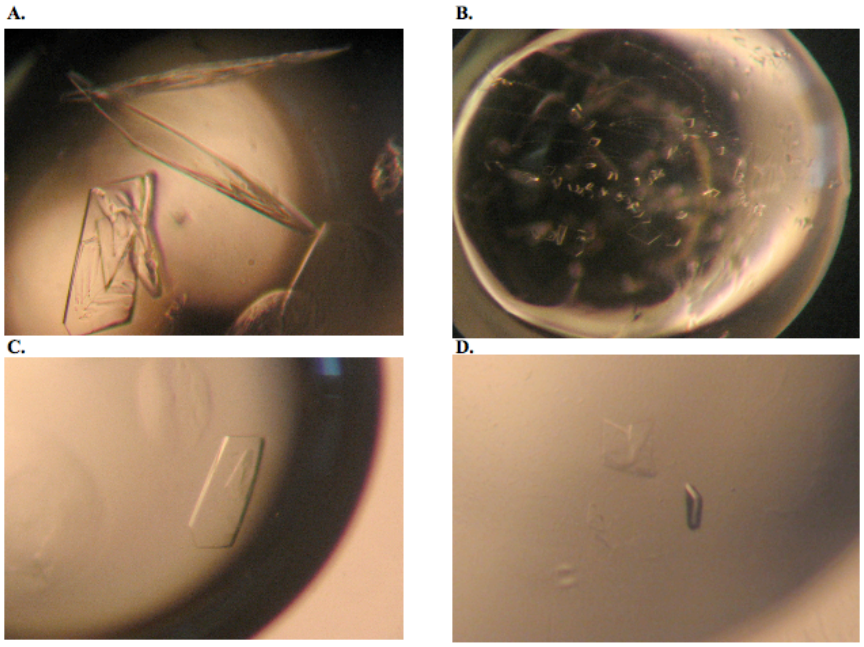

Figure 3.3.3. PER 229-575 V243D does not behave as PER 229-575: A. Gel sizing chromatogram of PER 229-575 V243D prepared and run under similar conditions to PER 229-575 depicted in Figure 3.3.1. There are more impurities and the protein peak contains two peaks. The first peak at 1.55 ml indicates a dimer-monomer equilibrium and the second peak at 1.61 ml indicates a monomer. B. SDS PAGE analysis of the affinity purified protein (Lane 1) shows impurities including a 59 kD protein consistent with a heat shock protein identified in other preparations. Lanes 2-12: fractions of the protein peak show two populations of protein, one full length (indicated by upper arrow) and the other slightly degraded (indicated by lower arrow). The degraded protein elutes at a volume consistent with the molecular weight of the monomer (38kD).

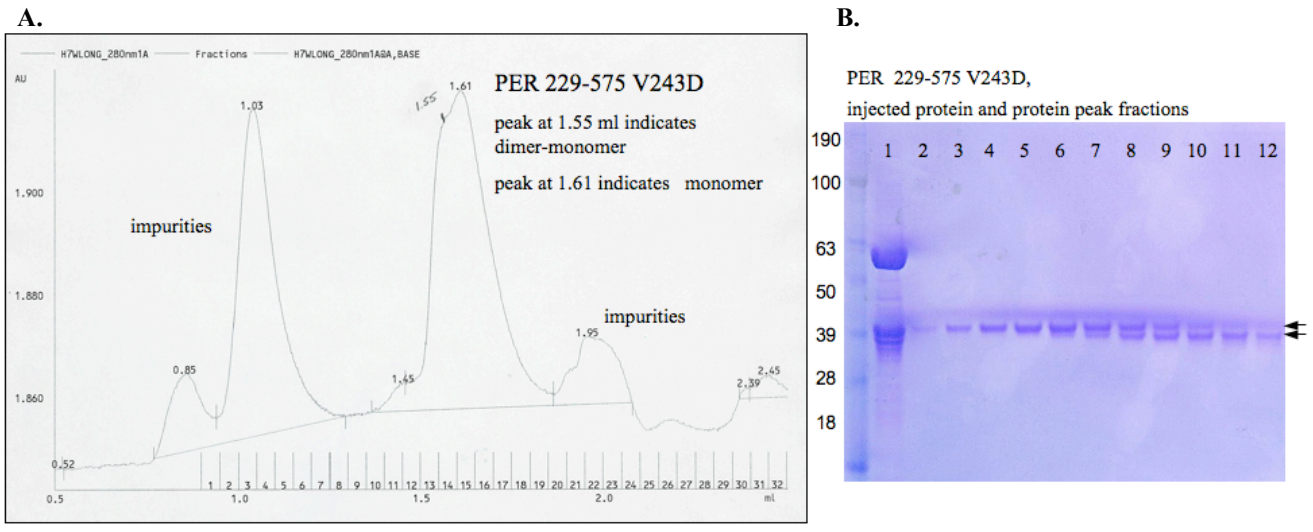

Conclusion:

PER 229-575 forms a dimer in solution. This protein crystallizes readily at room temperature overnight in the condition described in Part 2. The per^{Long} point mutation, V243, disrupts dimerization of PER 229-575 and destabilizes the protein. The undegraded V243D protein elutes from gel sizing columns at a volume consistent with a monomer-dimer equilibrium while the degraded band runs as a monomer. PER 229-575 V243 cannot be readily crystallized using the condition found for 229-575 or traditional screens.

PART 4: THE CRYSTAL STRUCTURE OF THE PER PAS DOMAIN REGION (229-575)

The crystal structure of the PER PAS domain region includes the PAS A domain, the PAS B domain, and two helices that extend beyond the PAS domains referred to as αE and αF. Each of the PAS domains seen in the structure follows the standard PAS fold as described in Part 1 (Figure 1.5), and can be described using the standard nomenclature.

Figure 4.1. The PAS fold seen in the PAS A & B domains of the PER PAS region. A. The PAS domain from HERG as depicted in [68] . B. The PER PAS B fold from this structure. C. The PER PAS A fold from this structure.

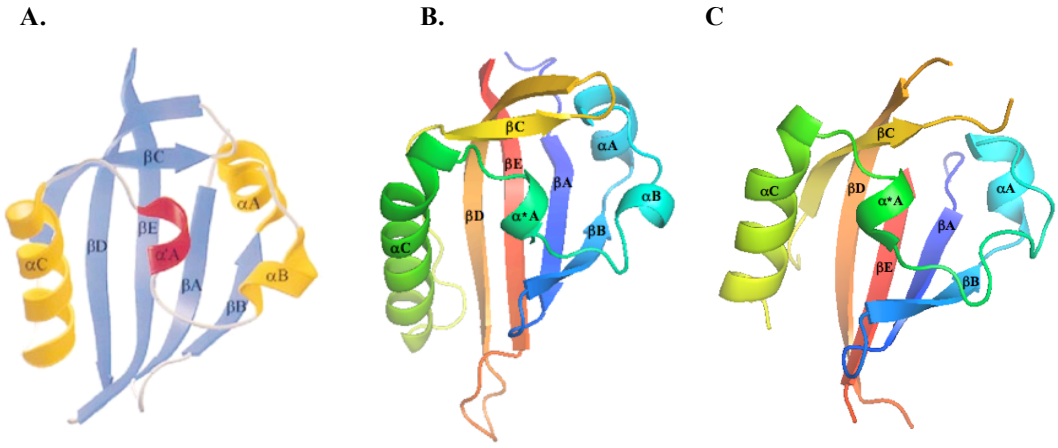

4.1: The asymmetric unit

The asymmetric unit is comprised of eight molecules arranged in four nearly identical dimer pairs (AB, CD, EF, and GH). Although the structure was solved in the P1 symmetry group, it has near monoclinic symmetry that can be seen in the near 90 angles of the β and γ cell dimensions (α=88.2°, β=89.6°, γ=89.9°). Systematic absences in the structure factors implies a screw axis, which can be observed in the relationship between dimer pairs. However, the structure could not be solved in P2 using the native data set.

Figure 4.1.1. The four dimers of the asymmetrical unit. The red/blue dimer pair can nearly be transposed over the green/yellow dimer pair

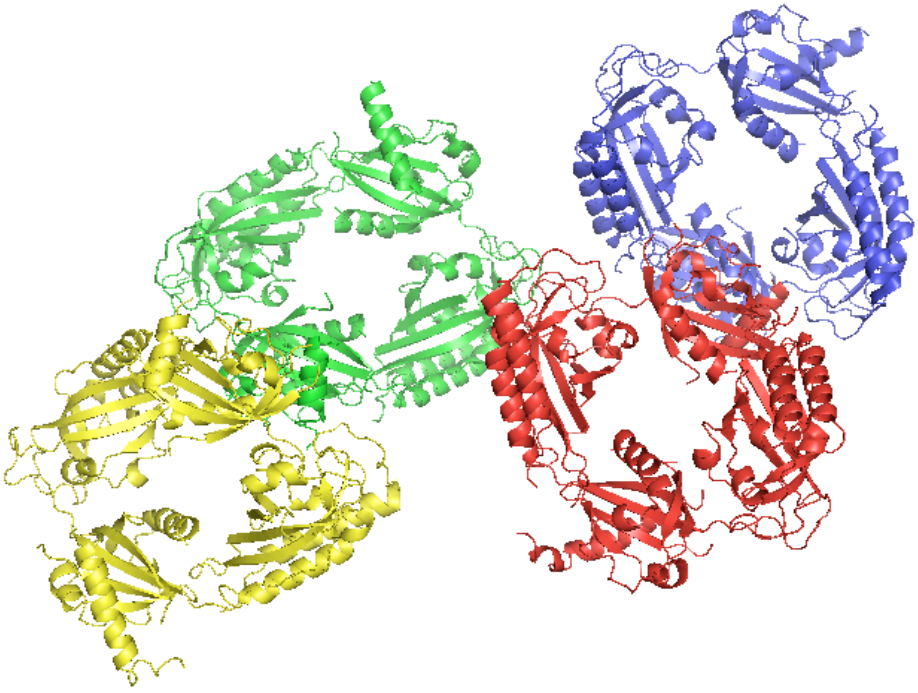

4.2: The dimer unit

The basic unit of the PER PAS domain region structure is a dimer consisting of four PAS domains. As described in Part 1, each PAS domain consists of four helices sitting atop a 5-strand beta sheet. The PAS A and B domains of each molecule are connected by a loop, and the second PAS domain is followed by two helices. Unlike a previously published structure of the PER PAS region, which shows an octamer of four joined dimers, this structure shows dimers that are self-contained and held together by symmetrical dimerization interactions. These include intramolecular and intermolecular PAS-PAS interactions and an interesting intermolecular interaction between PAS A and a helix from outside the PAS domain region.

Figure 4.2.1. Comparison of this structure versus another [1]. A. In this structure, PER dimers are held together by symmetrical PAS-PAS interactions and helix/PAS A interactions. Note the proximity of the N terminus (residue 236) of one molecule to the C terminus (residue 571) of the other, consistent with the possibility of an interaction between the N-terminus and residues 570-600. B. In [1], only one helix/PAS A interaction takes place and the other helix and PAS A surface participate in interactions with other pairs to form an octamer. C. The octamer depicted in [1].

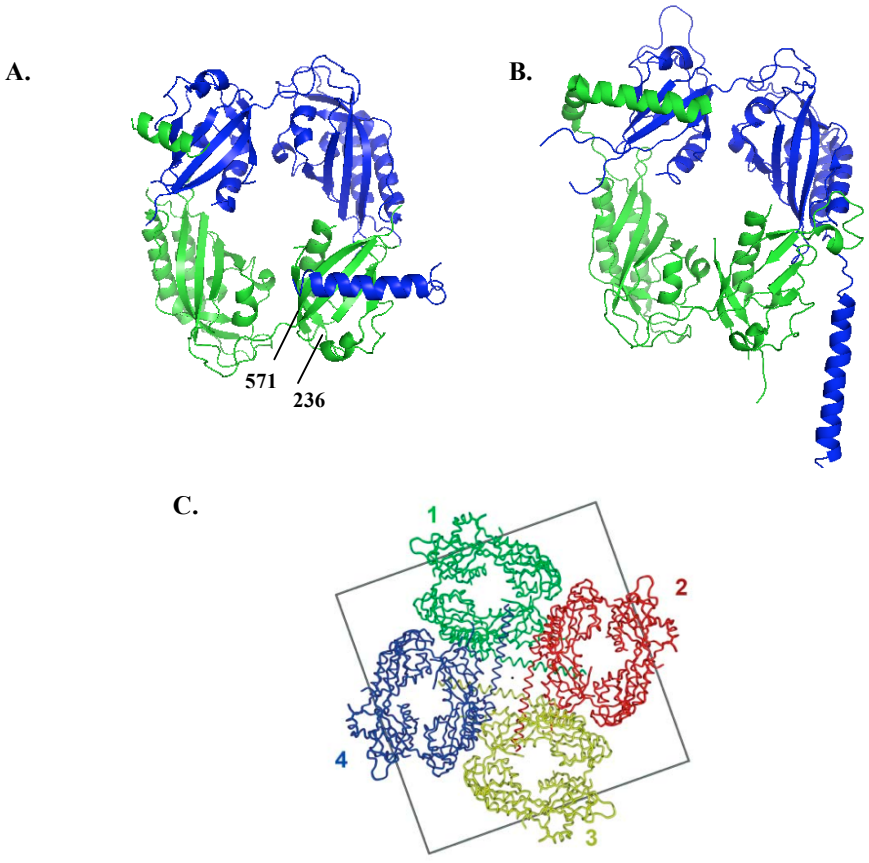

4.3: PAS-PAS intermolecular interactions

The four PAS domains of the dimer sit in a ring with hydrophobic interactions between the PAS A domain of molecule 1 and the PAS B domain of molecule 2 that are repeated between the PAS B domain of molecule 1 and the PAS A domain of molecule 2. These hydrophobic interfaces occur between a highly conserved tryptophan (W482) in the PAS B domain βD-βE loop and a pocket on the helical face of the PAS A domain of the partner molecule containing Glycine (G248), Serine (S273), and Isoleucine (I275). Similar interactions are seen in the previous structure. The tryptophan (W482) is conserved in other PERs, mPERs1-3, CYC, BMAL1, and mCLK. In *Drosophila* CLK, phenylalanine (F) replaces W482. In other tandem PAS domain proteins, such as AHR, Arnt, and SIM, this tryptophan is not conserved. The PAS A interacting residue G248 is also highly conserved. S273 and I275 are not as highly conserved.

Figure 4.3.1. Detailed view of the PAS-PAS symmetrical intermolecular interaction between W482 and G248, S273, and I275 from dimer GH. A. The location of the detail relative to the dimer. B. Detailed view of W482 from the βD-βE loop of PAS B in the pocket including G248, S273, and I275 made by the adjacent PAS A domain. Dots represent van der Waals surfaces.

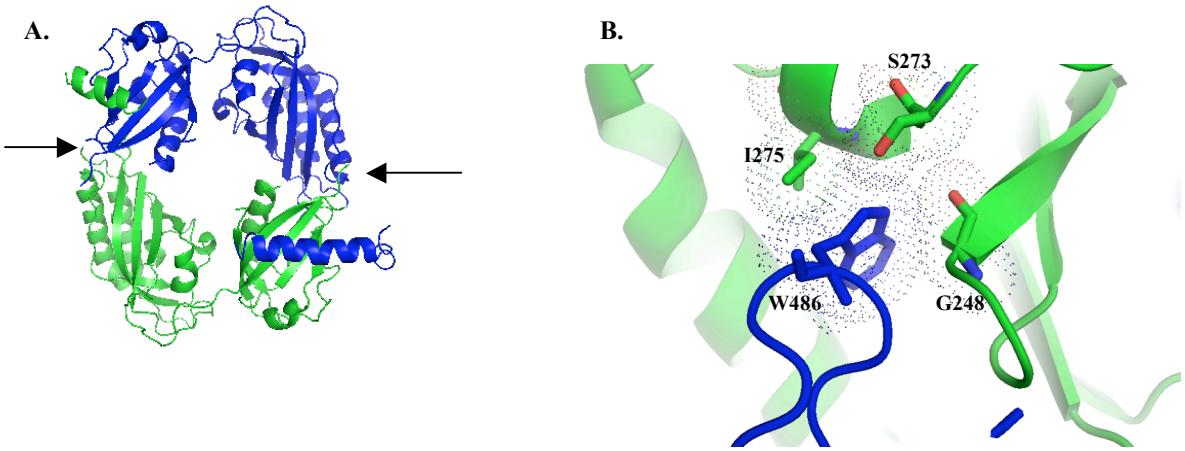

4.4 PAS A/αF intermolecular interactions

Helix F (αF) extends across the PAS dimer ring from the C-terminal end of one molecule to the PAS A beta sheet of the other, forming a key intermolecular interface based on interactions between hydrophobic residues on the PAS A beta sheet and αF. When αF is deleted (229-512), the PAS domain region fragment (PER 229-575) runs as a monomer on gel filtration [1]. The participating hydrophobic residues on the PAS A beta sheet lie in a row across the strands. They are Tyr 253 (on βB), Valine 243 (on βA), Valine 367 (on βE), and Valine 343 (on βD). A disulfide bond between Cys241 and Cys369 bridges the βA and βE strands and sits beneath αF.

Figure 4.4.1. The F helix interacts with the PAS A domain of the partner molecule to form a large hydrophobic interface: A. Overview of the dimer with arrows indicating the Pas A/ F helix interactions, B. Close up of the F helix of molecule B against the Pas A beta sheet of molecule A, C. F-helix residues involved in the interaction, D. PAS A residues involves in the interaction.

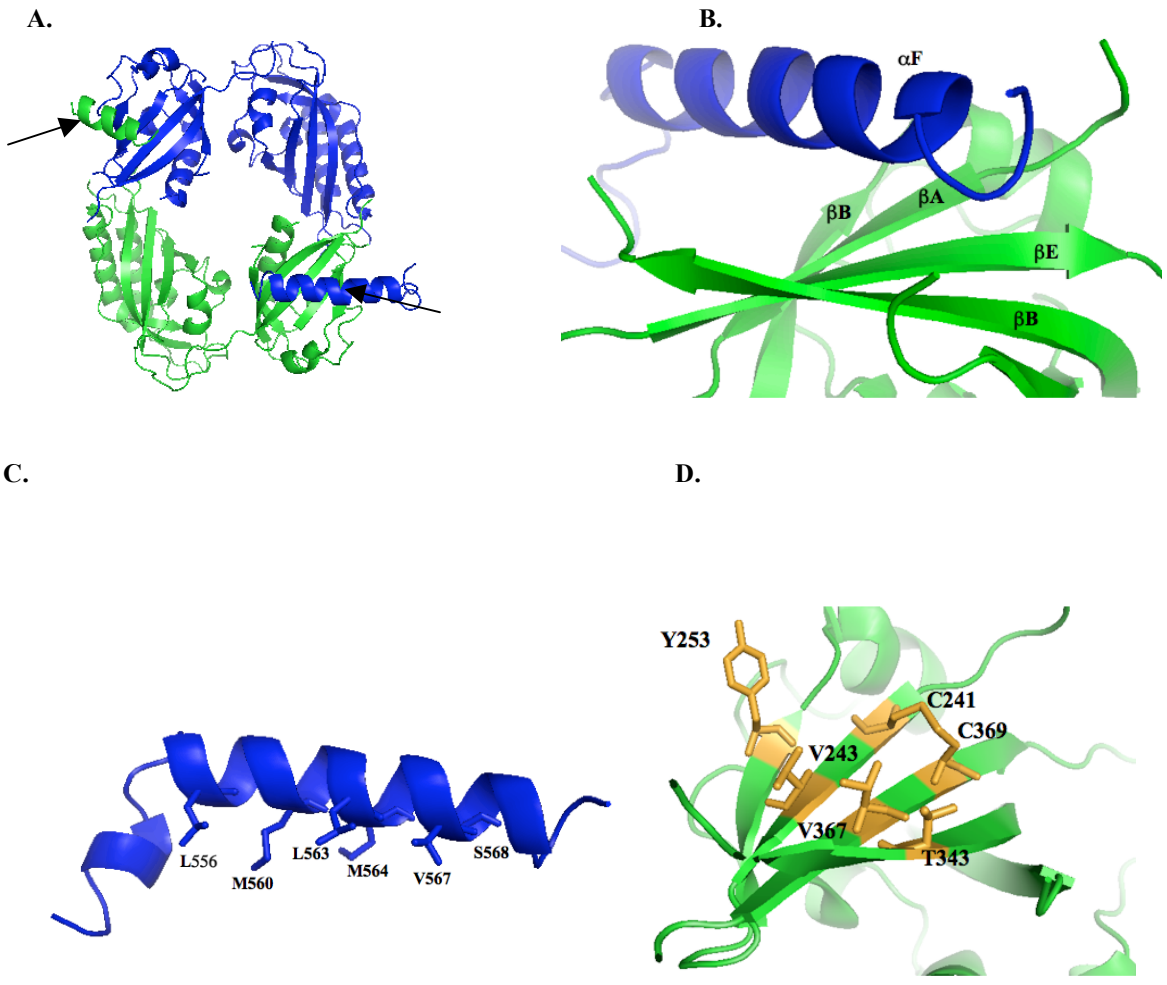

4.5 Flexibility in the PAS A/αF interaction

The structure reported here shows a symmetrically closed dimer, with both F helices bending in to lie across the PAS A domain of the dimerizing partner. This is unlike the previous structure in which the F helix of one molecule does not bend in but sticks out straight to bind the PAS A domain of another dimer pair in a manner that groups dimers into octamers. Although both F helices form similar intermolecular dimerization interfaces in the dimer, there are differences in the position of the helix on the beta sheet. The same key residues (shown in Figure 4.4.1) participate. However, the helix on one side of the dimer appears shifted one turn relative to the PAS A beta sheet. The difference in helical positions is consistent in each of the four dimers.

Figure 4.5.1. Differences between the two PAS A/ αF interactions of the dimer shown in molecule A and molecule B. For simplicity, only V243 is highlighted on the PAS A beta sheet A. Each of the four dimers has one PAS A/αF interaction wherein the central PAS A hydrophobic residue, Val243, sits between Met560 and M564 B. The second PAS A/αF conformation shows V243 flanked by Leu556 and M560.

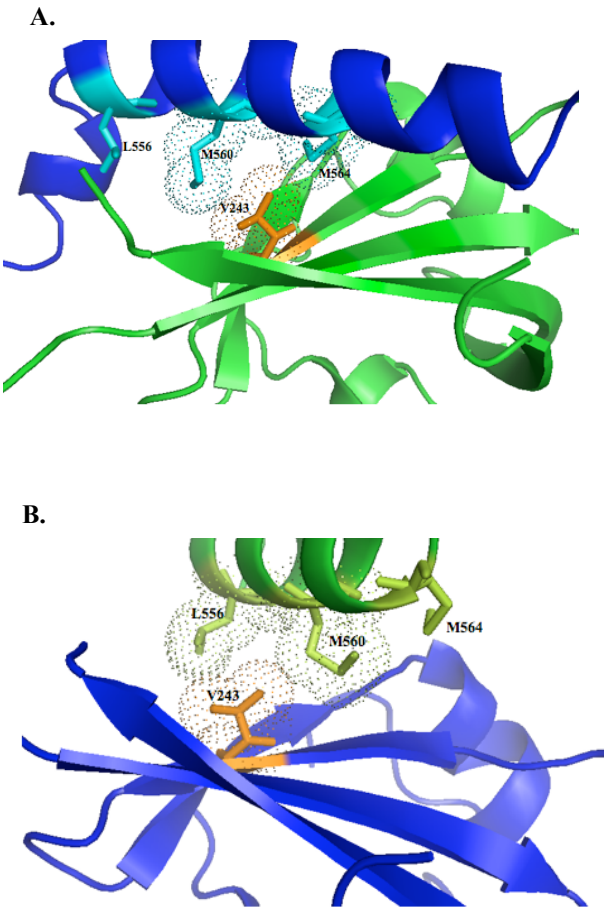

4.6 The position of the *per*^{Long} point mutation residue (V243)

The residue V243 sits at the center of the hydrophobic intermolecular PAS A/αF interaction. A close look at the interactions between this residue and the interacting F helix residues (in both positions described above) indicates that mutation of this Valine to Aspartic Acid would strongly disrupt the interaction. The observed effects of this mutation on PER 229-575 dimerization and stability in vitro is described in Parts 3 and 5.

Figure 4.6.1. Valine 243 (shown in orange) is a central residue in the PAS A/αF interaction

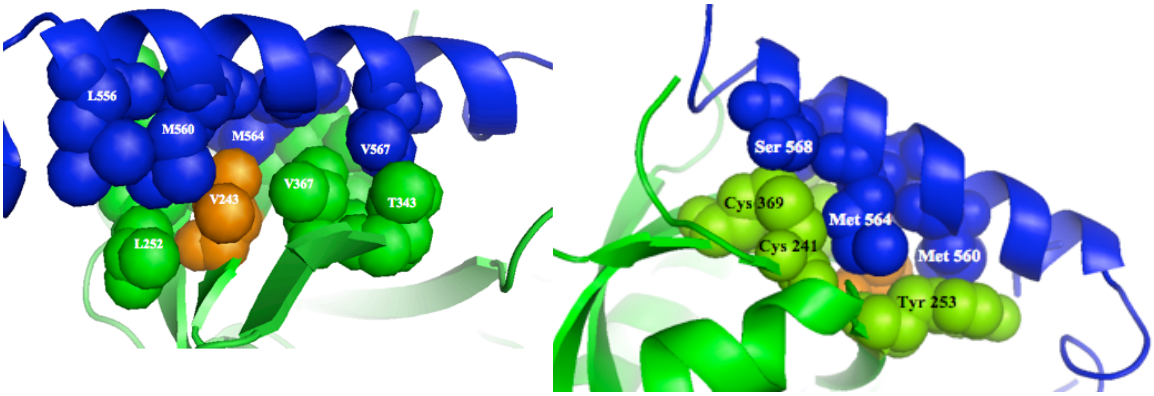

4.7 Residues associated with TIM binding and cytoplasmic localization

Some residues depicted in the PER 229-575 crystal structure have been identified previously as necessary for TIM binding. These include residues 233-390 (the PAS A domain) and residues 448-512 (the PAS B beta sheet) [83, 84].

Figure 4.7.1. Regions of PER 229-575 previously identified as necessary for TIM binding and cytoplasmic localization. A. Residues associated with binding TIM are highlighted in magenta.

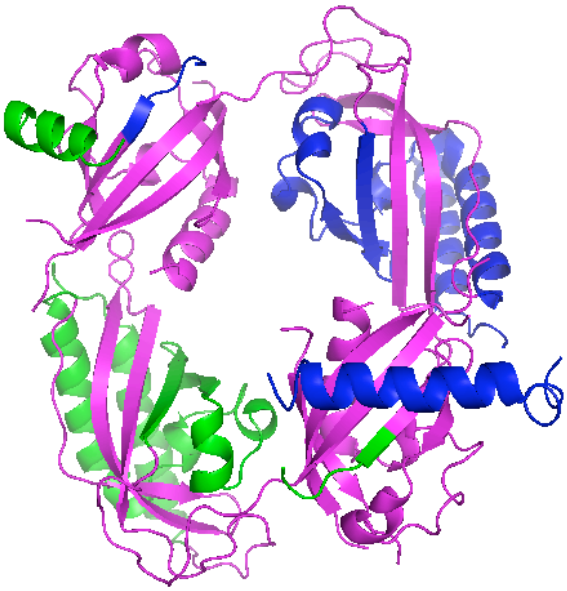

A PER fragment including the PAS AB domain region and beyond (233-685) and another PER fragment including only the PAS A domain (233-390) have been shown to bind TIM in yeast two-hybrid assays [83, 84]. GST pull downs of PER expressed in *E. coli* have also demonstrated interactions between these PER fragments and TIM. This indicates that TIM-binding residues in PER are near to and may overlap with residues of the PAS A beta sheet shown in the crystal structure to participate in the PAS A/αF interaction. It is interesting to consider the PAS A/αF interaction as one that may affect (and be affected by) PER-TIM binding. This is discussed further in Part 6.

The PAS B residues that bind TIM fragments in vitro (448-512) also act as a cytoplasmic localization domain (CLD) [83, 84]. In the absence of TIM, residues 448-512 keep otherwise nuclear PER in the cytoplasm. This is shown by the nuclear entry of PER Δ448-512 expressed in S2 insect cell culture (without TIM) versus wild type PER, which remains in the cytoplasm when expressed without TIM. It is proposed that the PER CLD binds some cytoplasmic element and that the binding interface is missing in

the PER Δ448-512 mutant and covered when PER binds TIM to prohibit the cytoplasmic interaction and promote nuclear entry. Because PER Δ448-512 is missing a critical structural element, its localization is difficult to interpret, and binding between 448-512 and Tim fragments *in vitro* involves isolated beta strands that may behave differently out of the context of the larger domain. The proposition, however, that the CLD (Pas B beta sheet) acts as a competitive binding interface is consistent with the typical role of the PAS beta sheet as a binding surface.

PART 5: Oligomerization of PER fragments in solution

The oligomeric state of a protein can be found by comparing the weight of the monomer as determined by SDS PAGE analysis to the weight of the native protein as indicated by its elution volume from a gel sizing column. All PER fragments selected for purification on a large scale (listed in Table 3.1) were run on such columns to determine their oligomeric state. None of these proteins eluted from the columns at volumes consistent with monomers, and most ran between trimer and tetramer size. Mutant versions of the PER 229-575 fragments were also assayed by this method. Mutations were designed to interfere with the PAS A/αF intermolecular interaction seen in the crystal structure. The effects of these mutations on the interactions between PER fragments in solution are consistent with the placement of mutated residues in the crystal structure.

5.1 Larger PER fragments behave as oligomers

Larger PER fragments, including 1-575, 1-700, 1-848, and even the slightly larger 147-573 run at elution volumes indicating molecular weights near

trimer size, rather than as dimers. These fragments may also be dimers that because of their structure run at a larger size. Consistent with this, larger fragments combined with 229-575 and run on gel sizing chromatography produce only one additional peak that exhibits a 1:1 ratio of proteins (see section 5.2). Proteins that include the N-terminus and end at 575 (1-575, 147-573) run even larger than those that include both the N-terminus and residues beyond 575 (1-700, 1-848), consistent with the possibility of a compacting interaction between the N-terminus and the region following 575, as discussed in section 3.2.

Figure 5.1.1. PER 1-575, 1-700, and 1-848 run as oligomers on Superdex 200 sizing columns. A. PER 1-575, a 63 kD protein, elutes from a Superdex 200 column at a volume consistent with a molecular weight of approximately 220 kD. B. PER 1-848, a 93 kD protein, runs at a volume consistent with a weight of approximately 360 kD. C. PER 147-575, a 47 kD protein, runs at a volume consistent with a weight of 165 kD.

A.

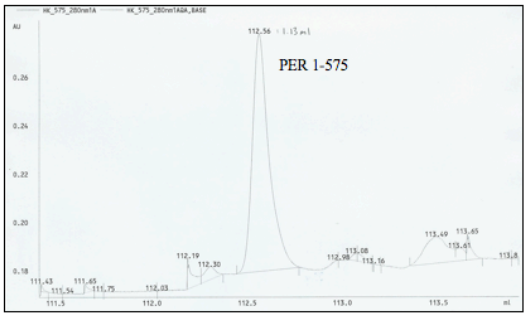

B.

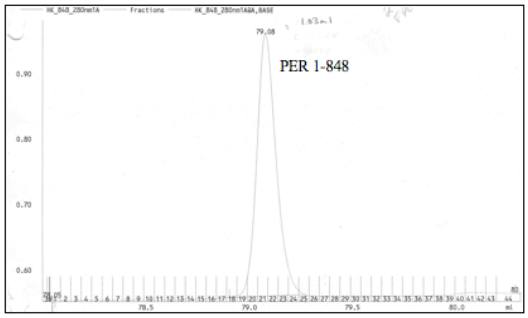

C.

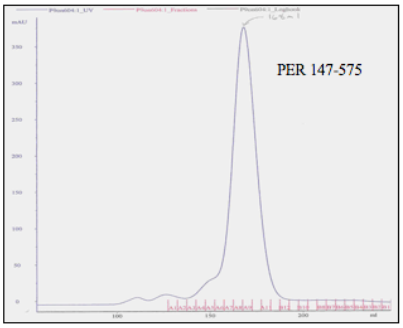

5.2 PER 229-575 runs near dimer size and recombines with larger fragments in a 1:1 ratio.

The PAS domain region fragment (229-575) runs close to dimer size, (see Figure 3.3.1). Larger fragments, when combined with the crystallized PAS region fragment (229-575), recombine into complexes with a 1:1 ratio, as shown by densitometry analysis of SDS PAGE peaks. A combined peak elutes from gel sizing columns in between the peak for the large protein and the 229-575 peak.

Figure 5.2.1. PER 229-575 forms complexes with larger PER fragments. A. PER 1-848 + PER 229-575 shows three peaks on a chromatogram B. SDS PAGE analysis shows the first peak is 1-848, the second peak is a combination of 229-575 and 1-848, and the third is 229-575. B. The same information as in A, but for a mixture of PER 1-575 and PER 229-575.

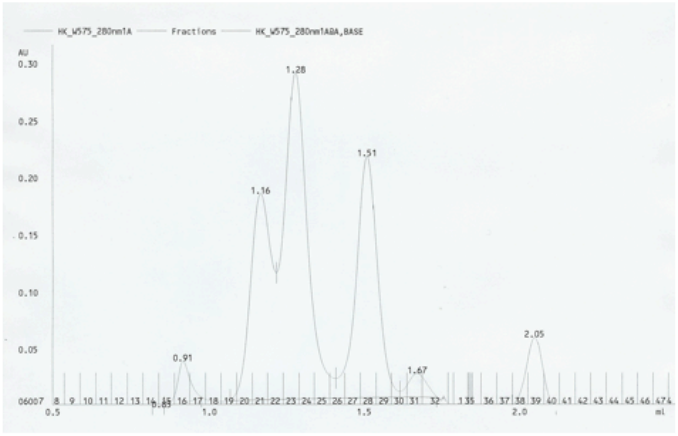

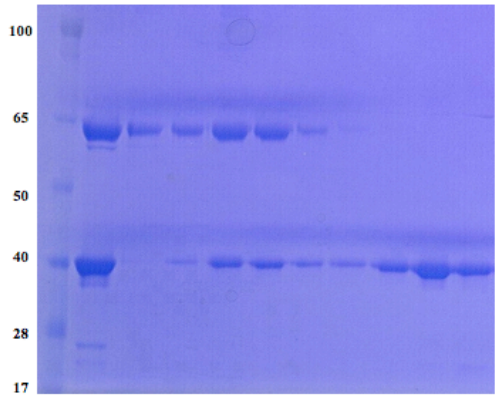

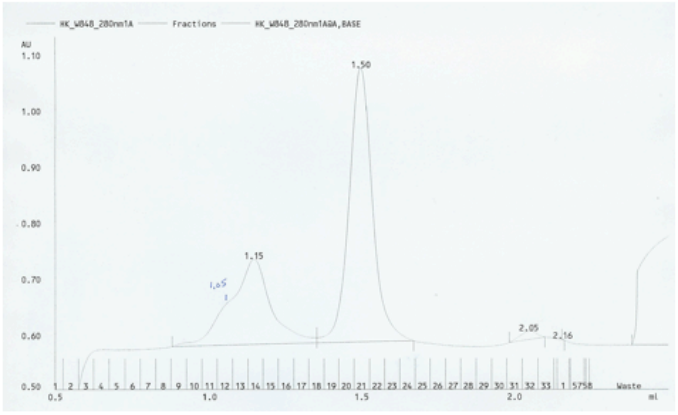

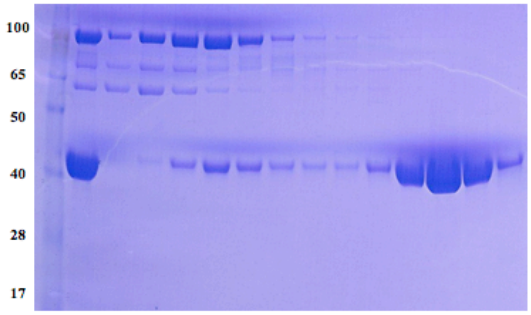

5.3 Mutations of residues involved in the PAS A/αF interaction observed in the crystal structure affect the monomer/dimer equilibrium of PER 229-575.

On the PAS A beta sheet, the V243D mutation inserts a large charged residue into the hydrophobic center, where αF of the interacting protein sits in the crystal structure. In solution, this mutation strongly hinders dimerization (see Part 3, Figure 3.3.3) and stability of PER 229-575.

On the F helix, the key hydrophobic residues that interact with the PAS A beta sheet of the interacting protein are L556, M560 and M564. As discussed in Part 4.5, αF is found in two positions. In position 1, L556 and M560 are the key interactive residues flanking V243 of the opposing beta sheet. In position 2, the M560 and M564 flank V243. Mutating any of these residues to alanine does not strongly affect the dimerization of PER 229-575 in solution. The shift of the protein peak toward monomer is minimal (an elution shift from 1.5 to 1.51 or 1.52 ml). Mutating M560 (which interacts withV243 in both observed positions) to alanine does not alter the position of the dimer peak but produces an unusual peak near the void volume of the

gel sizing column. Protein from this peak merits further investigation to determine whether it is a contaminant, such as heat shock protein, or a larger PER oligomer.

Figure 5.3.1. PER 229-575 αF mutants are not significantly affected in their monomer-dimer equilibrium. A. PER 229-575 elutes from a Superdex 200 sizing column at a volume consistent with the molecular weight of the dimer. B. PER 229-575 L556A behaves similarly. C. PER 229-575 M560A runs as a dimer, but a large peak near the void volume merits further investigation D. Per 229-575 M564A runs similarly to wild type and L556A.

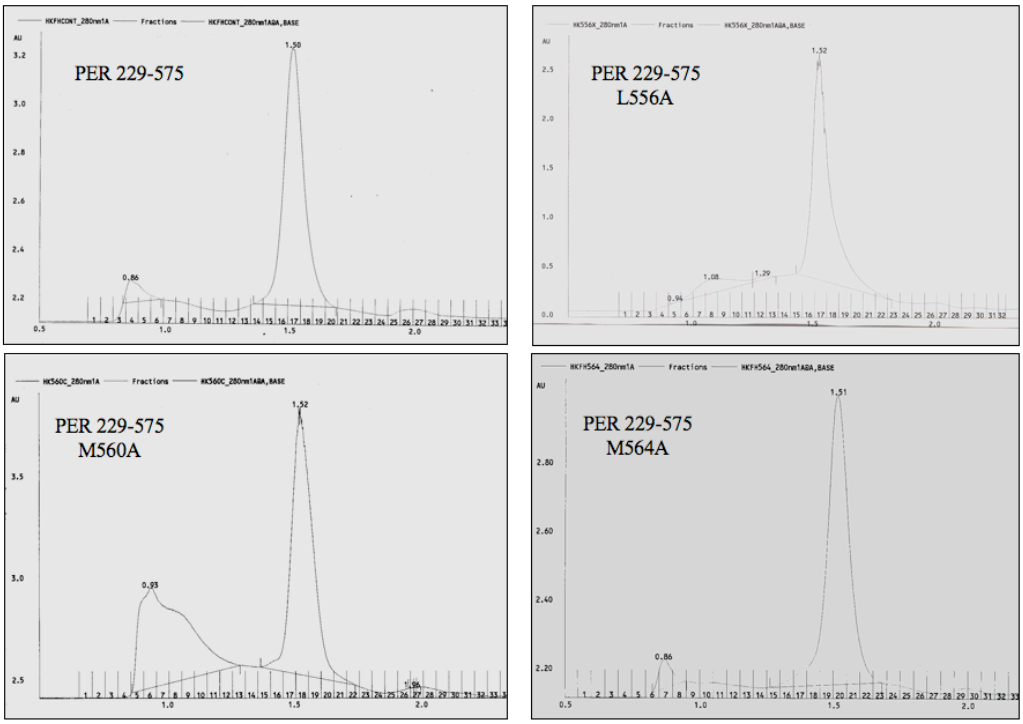

5.4 The monomer-dimer equilibrium of PER 229-575 in solution is affected by ionic strength.

In 50mM Tris pH7.5, 500mM NaCl, 2mM DTT, PER 229-575 runs as a dimer with an elution volume of 1.47ml. In the same buffer, with 150mM NaCl, some monomer is evident with a elution peak at 1.50 ml. Reducing the salt concentration of the buffer further monomerizes PER 229-575. The positive effect of ionic strength on dimerization suggests that dimerization in solution depends on hydrophobic interactions, such as those seen in the crystal structure. The higher concentration of the PER run in 150mM salt does not contribute to differences in elution volume. Changing the concentration of the protein, even by 20-fold, does not affect dimerization.

Figure 5.4.1. The molecular weight of PER 229-575 complexes in four different NaCl concentrations. Lines labeled “D” and “M” indicate peak volumes consistent with the dimeric and monomeric molecular weights. A. Per 229-575 in 50mM Tris pH7.5, 2mM DTT with 150 mM NaCl B. As in A, but with 120mM NaCl. C. As in A, but with 90 mM NaCl. D. As in A, but with 60mM NaCl.

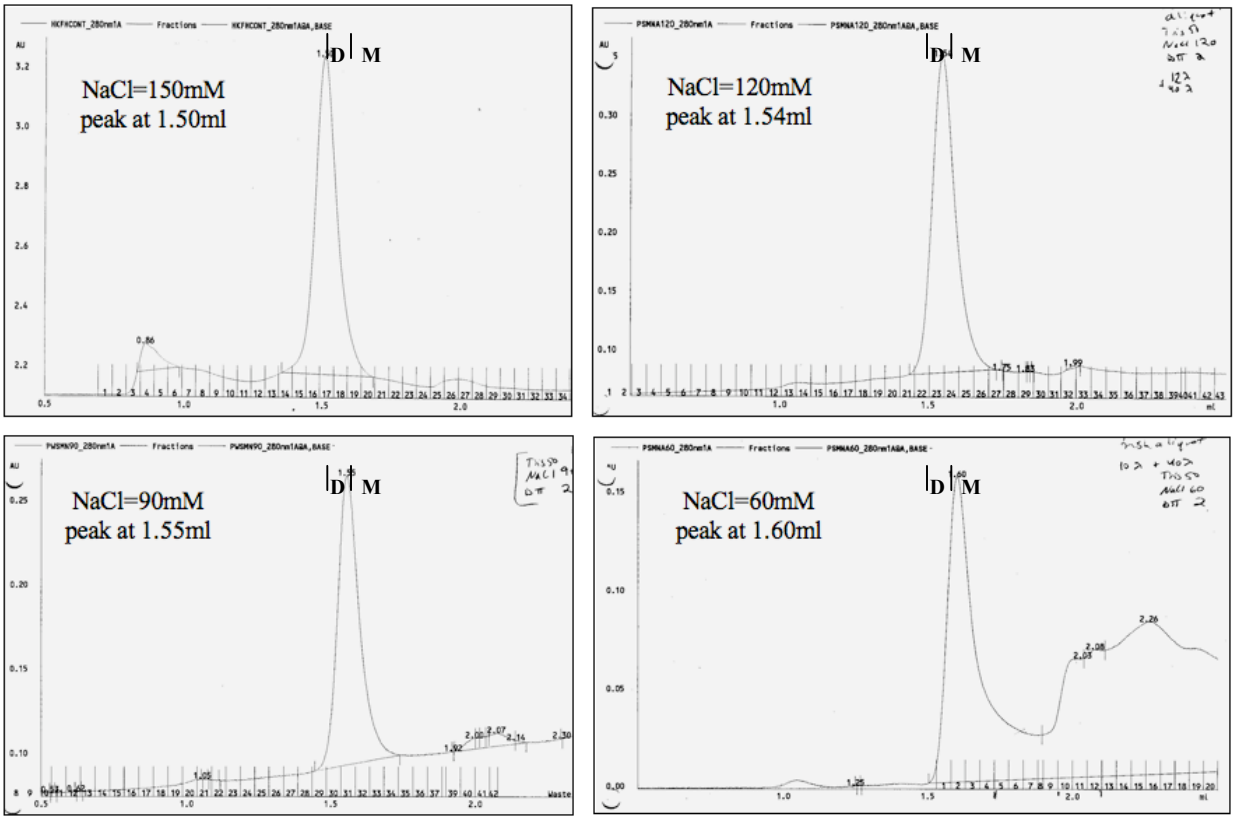

PART 6: Discussion

PER fragment purification

In the search for PER fragments that are both interesting and practical for purification in large quantities, the problem of nucleic acid binding should be considered. The nucleic acid remaining bound to PER 1-700 after purification appears to be RNA, but this may be a consequence of greater activity of the DNAse versus RNAse added during cell lysis. Eliminating nucleic acid binding can be accomplished by eliminating the N-terminal 87 residues of PER. However, this creates stability problems in PER fragments that extend beyond residue 575. Eliminating nucleic acid binding without introducing stability problems may be possible through specific internal deletions or mutations of basic N-terminal residues. Although it is possible that the same residues responsible for nucleic acid binding stabilize regions beyond residue 575, or that the binding of nucleic acid itself somehow stabilizes the protein, it is likely that nucleic acid binding residues could be safely eliminated. The stretch of basic residues which act as the PER nuclear localization sequence (NLS) is likely to mediate nucleic acid binding

[85]. These residues lie between 60 and 80 as follows: 61 SDMIIKRNKD KSRKKKKNKG 80. An internal deletion, Δ60-80, would eliminate these residues but conserve 1-60. Residues 1-15 of PER are highly conserved and may be responsible for stabilizing the PER region beyond 575, in which case the problems of both instability and nucleic acid binding could be eliminated.

Interactions between the PER N-terminus and the short/mutable region

The destabilizing effects of the Δ1-87 deletion on regions beyond residue 575 indicate the PER N-terminus may interact with the short/mutable region that lies between 575 and 600. The effect of Δ1-87 on the stability of 575-700, which appears to similarly affect 575-692 and 575-848, may also depend on a interaction between the N-terminus and some other region of PER that indirectly stabilizes the 575-600 region. In either case, a more detailed deletion/mutation analysis of residues 1-87 would allow a more precise characterization of the possible interplay between the N-terminus and short/mutable region of PER.

The PER PAS AB dimer

The PAS domain region of PER behaves as a dimer both in solution and in the crystal structure presented here. This dimer has four major intermolecular interfaces. The first two are between PAS domains and join the PAS A domain of the first molecule with the PAS B domain of the second and vice versa ($PASA_1$-$PASB_2$ and $PASA_2$-$PASB_1$). This creates a ring of PAS domains that follows the pattern $PASA_1$-$PASB_1$-$PASA_2$-$PASB_2$.

Figure 6.1. The PER PAS domain dimer is held together by two types of interactions (indicated by yellow asterisks). A. The PAS A-PAS B interface. B. The PAS A-αF interface

A. **B.**

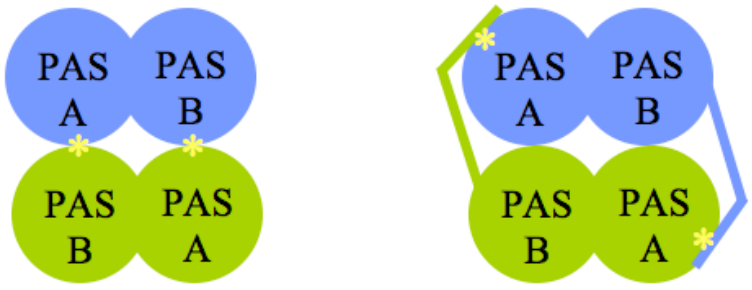

PER-PER interactions in a PER fragment containing the crystallized region (PER 233-685) have also been observed in yeast-two hybrid experiments and in *in vitro* pull down assays [86]. A weaker interaction between the PAS A domain of PER (PER 233-390) and a fragment including αF (PER 524-685) was also seen. Immunoprecipitation of full-length HA and Myc-tagged PER from fly head extracts also indicates that full-length PER expressed in flies self-binds, although in limited amounts [87].

Binding between larger PER fragments expressed *in vitro* (PER 1-848 and PER 1-575) and PER 229-575 indicates that the intermolecular interactions that hold together PER 229-575 dimers may be present in the larger fragments. The new complexes formed run at molecular weights between those of the larger protein complexes and the smaller 229-575 dimers . The ratio of large to small proteins in the new complexes is 1:1. These new complexes appear to represent dimers composed of one large and one small fragment.

Conservation of the PER PAS ring structure

The conservation of the PAS-PAS interacting residues of PER (W482, G248, S273 and I275) in other PAS A/B tandem repeat proteins, including CLK, CYC, mPERs1-3, mCLK, and BMAL1, indicates these proteins may also form the type of PAS dimer depicted in Figure 6.1 . Like PER, these PAS AB proteins may require additional intermolecular interfaces for dimerization. Because the F helix is not conserved beyond the insect PERs, this interaction is unlikely to act as the secondary interface. A secondary binding interface, if present in other PAS AB proteins, may be specific to the individual protein. Alternatively, the PAS-PAS interfaces of other PAS AB proteins may be sufficient themselves to dimerize the proteins.

The PAS A/αF intermolecular latching interaction

Although the PAS A/αF interaction is a critical dimerization interface in the PER PAS structure, it also appears to be more dynamic, as seen in its two positions in the structure presented here and in the third, outstretched position shown in the previous structure. It is interesting that the four dimers that make up the octamer in the previous structure are held together by a single PAS A/αF interaction, implying that only one such interaction is

required for dimerization. The loss of 2-3kD from PER 299-575 and, to a much greater extent, from PER 229-575 V243D, is consistent with the loss of the F-helix beyond the bend (around residue R551). If the F-helix can move into multiple positions, it may be more susceptible to proteolytic cleavage.

It is interesting to consider whether the accessibility and the flexibility of the F helix are recapitulated to some degree in full-length PER *in vivo*. This could facilitate access to residues at or around those involved in the hydrophobic interface by modifying proteins such as kinases. Phosphorylation of helix residues S550, S558, T562, or S568, or of the PAS residues Y253 or T343, which sit beneath the helix, could affect the larger PER-DBT-TIM complex by reducing PER dimerization.

The *per*^{Long} residue (V243)

One example of how a large, negatively charged group inserted into the observed PAS A /F hydrophobic interface affects PER self-association is seen in PER 229-575 V243D. This mutation has two major effects on PER 229-575. First, it interrupts the PER-PER interaction. This can be seen by

the shift of the peak protein on gel sizing that indicates an increasingly monomeric protein. Second, it increases the 2-3kD degradation of PER. In V243D, the smaller "under band" is far more prevalent, and it runs as a strict monomer on gel sizing. Wild-type PER 229-575 that has degraded in this manner continues to run as a single dimer peak on gel sizing columns, so that the loss of 2-3kD in V243D does not alone account for monomerization. The compromised, though not completely destroyed, dimerization interaction of V243D in solution is consistent with the crystal structure, because the insertion of an aspartic acid into the PAS A/αF interface would likely destabilize the interaction.

The F helix

Mutations to the key interactive residues of the F-helix (L556A, M560A, and M564A) also produce results consistent with the crystal structure. In solution, these mutations do not significantly affect dimerization or stability of the PER 229-575 fragment. In the structure, two positions are observed, that may be allowed by the repeated hydrophobic motifs at the three key helical turns (555Q**A<u>L</u>**AS**F<u>M</u>**ET**L<u>M</u>**D565). Only two turns of the helix participate significantly in the hydrophobic interaction with PAS A, and

these can be either L556 and M560 (Position 1) or M560 and M564 (Position 2). It also appears that a twist of the helix would not significantly disrupt the hydrophobic interface, because L556, M560, and M564 are each proceeded by other hydrophobic residues.

The *per*^{Long} mutation (V243D)

The biochemical effects of V243D on the PER 229-575 fragment in solution and the position of V243 in the 229-575 crystal structure are interesting to consider in light of the known *in vivo* effects of this mutation, known as *per*^{Long}. This mutation was one of the original circadian mutants characterized, and its effects on the circadian rhythm of flies has been well documented [11]. The primary effect of *per*^{Long} is to delay nuclear entry of PER and TIM, thereby slowing the period of the clock. It was once speculated that *per*^{Long} delayed nuclear entry by disrupting the PER-TIM interaction, because the *per*^{Long} mutation is located in the PAS A domain of PER, which is also known to be involved in TIM binding [84]. The opposite was found to be true, however; *per*^{Long} enhanced PER-TIM binding in Yeast two-hybrid experiments [84]. Studies have also shown that per^{Long} does not diminish the stability of PER *in vivo*, nor does it delay formation of

PER/TIM complexes [23, 87]. The yeast two-hybrid result, though positive, does suggest some effect of *per*^{Long} on the PER TIM interaction, but one that is subtler than simple disruption or delay. This effect may delay the release of PER from TIM, an event now recognized as a part of nuclear entry and one that delayed in *per*^{Long} [23].

PER-TIM binding and the PER PAS region

One model to explain the effects of V243D on PER-TIM binding as well as the PAS A/αF interaction is one in which the PASA/αF dimerization interaction stabilizes PER during its release from TIM prior to nuclear entry. If the PER-TIM interaction (known to involve the PER PAS A domain) occupies residues adjacent to or overlapping with the PAS A residues that bind αF, the F helix may not rest on the PAS A beta sheet, as it does in the structure, when PER is bound to TIM. The release of PER from TIM, however, may be stabilized by this interaction. This scenario is depicted in Figure 6.2.

Figure 6.2. A model of how the PAS A/αF dimerization interaction might facilitate the release of PER from TIM that is part of nuclear entry. Dimerization of PER facilitates release from TIM by stabilizing free PER. A compromised dimerization interface, as in V243D, in this case, would hamper the release of PER and delay nuclear entry.

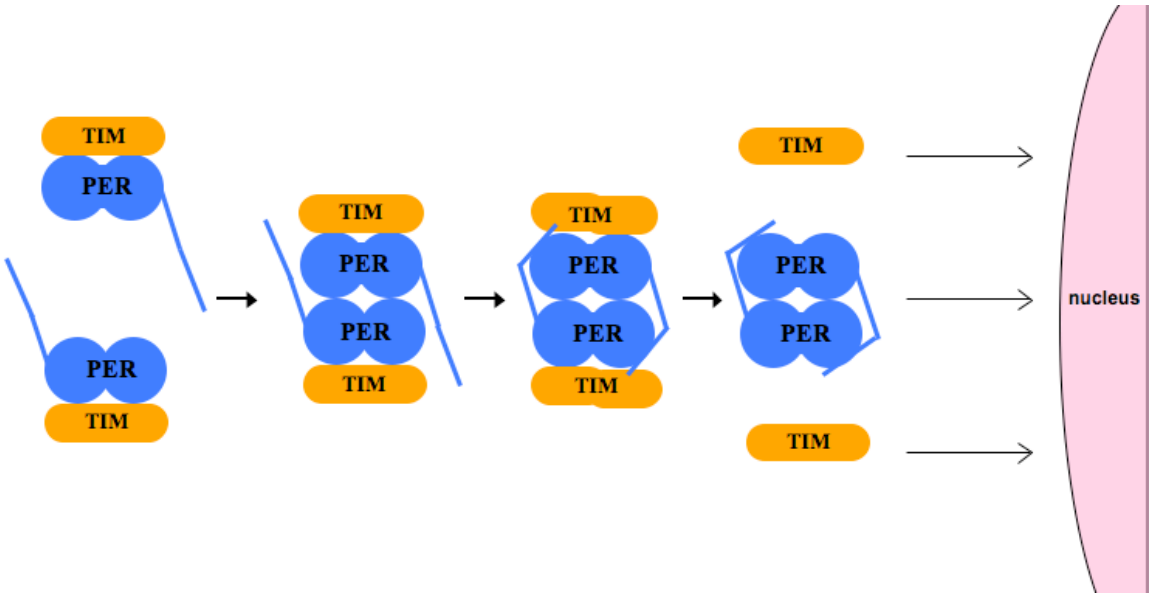

Considering V243D as a mutation that may disrupt the release of PER from TIM may help explain past observations of an enhanced interaction between PER and TIM with V243D at ambient temperatures [84]. This train of thought is only possible in light of new information about the separation of PER from TIM that occurs during nuclear entry. The flexible F helix may

be able to both reveal and cover the PAS A beta sheet in order to move PER in and out of a larger complex with TIM. A more thorough investigation of this interaction based on the study of full length PER expressed in flies or cell culture will improve our understanding of the importance of the dimerization interfaces seen in the crystal structure presented here and their potential effects in PER interactions *in vivo*.

Testing the *in vivo* effects of an altered PAS A/αF interaction

The *in vivo* effects of a mutation that interrupts the hydrophobic surface of the PAS A beta sheet (V243D) have been described in several publications, and include a lengthened circadian rhythm associated with a delay in the nuclear entry of PER, as well as further lengthening of the circadian period and arrhythmicity with increased temperatures. These effects, however, may be caused by effects on interactions other than the self-binding PAS A/αF interaction seen in the crystal structure. A deletion mutation that eliminates the F helix (*per*$^{\Delta C}$, which lacks residues 515-568) has also been described [88]. This deletion causes a number of effects including delayed nuclear entry, lengthening of the circadian period with increased temperature, reduced amplitude oscillations of PER, PER hypophosphorylation, and

decreased degradation of PER in response to light. Because the overall structure of the protein would be changed by the 515-568 deletion, it is difficult to relate its effects directly to an altered PER PAS A/αF interaction. Similar problems would arise from other mutations designed to destroy or hinder the PAS A/αF interaction. Another method to test the affects of this interaction on PER would be to lock the interaction by engineering a disulfide bridge between the PAS A beta sheet and the F-helix to fasten the helix into a closed position. Paired mutations, such as V243C and M560C, could be first tested as strongly dimerizing or "locked" *in vitro* by chromatographic analysis and crystal structure determination of the 229-575 fragment bearing the cysteine mutations. Observation of full-length PER expressed in flies or cell culture and carrying such mutations may also reveal increased PER homodimerization. If PER homodimerization is significantly increased *in vivo*, associated effects on PER-TIM binding or PER nuclear entry could also be examined.

Summary

The dimerizing interactions between PER proteins revealed in the crystal structure and chromatographic analyses presented in this work demonstrate a mechanism for protein-protein interactions between tandem PAS domain proteins. These interactions create a ring of four PAS domains latched together by dynamic interactions involving an helix outside the PAS domains (the F helix). Based on the sequence conservation of residues involved in intra-protein and inter-protein interfaces of the ring, this type of structure may also occur in the PER proteins of other species and in other tandem PAS proteins. The latching interaction, however, is not conserved beyond insects and may provide a unique means of regulating the dimerization of insect PERs. This interaction is strongly hindered by the per^{L} (V243D) mutation, which is known to lengthen circadian rhythms in flies by delaying the nuclear entry of PER. It has been shown that the per^{L} mutation does not destabilize PER or hinder the formation PER-TIM complexes [23, 86]. It is possible that per^{L} may affect the same interaction *in vivo* seen in the crystal structure, a PER-PER interaction. If this PER-PER interaction stabilizes the release of PER from TIM that occurs prior to nuclear entry, this could help explain the delay in nuclear entry seen in per^{L}

flies. Tests to demonstrate PER homodimerization *in vivo* and its relationship to the separation of PER from TIM a nuclear would inform this model.

REFERENCES:

1. Yildiz, O., et al., *Crystal structure and interactions of the PAS repeat region of the Drosophila clock protein PERIOD.* Mol Cell, 2005. **17**(1): p. 69-82.

2. Baylies, M.K., et al., *Changes in abundance or structure of the per gene product can alter periodicity of the Drosophila clock.* Nature, 1987. **326**(6111): p. 390-2.

3. Curtin, K.D., Z.J. Huang, and M. Rosbash, *Temporally regulated nuclear entry of the Drosophila period protein contributes to the circadian clock.* Neuron, 1995. **14**(2): p. 365-72.

4. Jay C. Dunlap, J.J.L., Patricia J. Decoursey *Chronobiology: Biological Timekeeping* 2003: Sinauer Associates.

5. Zucker, I., *Chronobiology and Neuroscience.* Science, 1983. **220**(4599): p. 854-855.

6. Zimmerman, W.F., C.S. Pittendrigh, and T. Pavlidis, *Temperature compensation of the circadian oscillation in drosophila pseudoobscura and its entrainment by temperature cycles.* J Insect Physiol, 1968. **14**(5): p. 669-84.
7. Pittendrigh, C.S., *Temporal organization: reflections of a Darwinian clock-watcher.* Annu Rev Physiol, 1993. **55**: p. 16-54.

8. Pittendrigh, C.S., *Circadian rhythms and the circadian organization of living systems.* Cold Spring Harb Symp Quant Biol, 1960. **25**: p. 159-84.

9. Page, T.L., P.C. Caldarola, and C.S. Pittendrigh, *Mutual entrainment of bilaterally distributed circadian pacemaker.* Proc Natl Acad Sci U S A, 1977. **74**(3): p. 1277-81.

10. Richter, C.P., *"Dark-active" rat transformed into "light-active" rat by destruction of 24-hr clock: function of 24-hr clock and synchronizers.* Proc Natl Acad Sci U S A, 1978. **75**(12): p. 6276-80.

11. Konopka, R.J. and S. Benzer, *Clock mutants of Drosophila melanogaster.* Proc Natl Acad Sci U S A, 1971. **68**(9): p. 2112-6.

12. Feldman, J.F. and M.N. Hoyle, *Isolation of circadian clock mutants of Neurospora crassa.* Genetics, 1973. **75**(4): p. 605-13.

13. Bargiello, T.A. and M.W. Young, *Molecular genetics of a biological clock in Drosophila.* Proc Natl Acad Sci U S A, 1984. **81**(7): p. 2142-2146.

14. Jackson, F.R., et al., *Product of per locus of Drosophila shares homology with proteoglycans.* Nature, 1986. **320**(6058): p. 185-8.

15. Ewer, J., et al., *Requirement for period gene expression in the adult and not during development for locomotor activity rhythms of imaginal Drosophila melanogaster.* J Neurogenet, 1990. **7**(1): p. 31-73.

16. Siwicki, K.K., et al., *Antibodies to the period gene product of Drosophila reveal diverse tissue distribution and rhythmic changes in the visual system.* Neuron, 1988. **1**(2): p. 141-50.

17. Dunlap, J.C., *Closely watched clocks: molecular analysis of circadian rhythms in Neurospora and Drosophila.* Trends Genet, 1990. **6**(5): p. 159-65.

18. Dunlap, J.C., *Molecular bases for circadian clocks.* Cell, 1999. **96**(2): p. 271-90.

19. Shearman, L.P., et al., *Two period homologs: circadian expression and photic regulation in the suprachiasmatic nuclei.* Neuron, 1997. **19**(6): p. 1261-9.

20. Harmer, S.L., S. Panda, and S.A. Kay, *Molecular bases of circadian rhythms.* Annu Rev Cell Dev Biol, 2001. **17**: p. 215-53.

21. Allada, R., *Circadian Clocks: A Tale of Two Feedback Loops.* Cell, 2003. **112**(3): p. 284-286.

22. Roennenberg, T. and M. Merrow, *The Network of Time: Understanding the Molecular Circadian System.* Curr Biol, 2003. **13**: p. R198-R207.

23. Meyer, P., L. Saez, and M.W. Young, *PER-TIM interactions in living Drosophila cells: an interval timer for the circadian clock.* Science, 2006. **311**(5758): p. 226-9.

24. McClung, C.R., B.A. Fox, and J.C. Dunlap, *The Neurospora clock gene frequency shares a sequence element with the Drosophila clock gene period.* Nature, 1989. **339**(6225): p. 558-62.

25. Millar, A.J., et al., *The regulation of circadian period by phototransduction pathways in Arabidopsis.* Science, 1995. **267**(5201): p. 1163-6.

26. Tsinoremas, N.F., et al., *A sigma factor that modifies the circadian expression of a subset of genes in cyanobacteria.* EMBO J, 1996. **15**(10): p. 2488-95.

27. Whitmore, D., et al., *Zebrafish Clock rhythmic expression reveals independent peripheral circadian oscillators.* Nat Neurosci, 1998. **1**(8): p. 701-7.

28. Tei, H., et al., *Circadian oscillation of a mammalian homologue of the Drosophila period gene.* Nature, 1997. **389**(6650): p. 512-6.

29. Young, M.W., *Life's 24-hour clock: molecular control of circadian rhythms in animal cells.* Trends Biochem Sci, 2000. **25**(12): p. 601-6.

30. Cheng, P., et al., *Regulation of the Neurospora circadian clock by an RNA helicase.* Genes Dev, 2005. **19**(2): p. 234-41.

31. Elvin, M., et al., *The PAS/LOV protein VIVID supports a rapidly dampened daytime oscillator that facilitates entrainment of the Neurospora circadian clock.* Genes Dev, 2005. **19**(21): p. 2593-605.

32. Rothenfluh, A., M.W. Young, and L. Saez, *A TIMELESS-independent function for PERIOD proteins in the Drosophila clock.* Neuron, 2000. **26**(2): p. 505-14.

33. Lee, C., K. Bae, and I. Edery, *PER and TIM inhibit the DNA binding activity of a Drosophila CLOCK-CYC/dBMAL1 heterodimer without disrupting formation of the heterodimer: a basis for circadian transcription.* Mol Cell Biol, 1999. **19**(8): p. 5316-25.

34. Price, J.L., et al., *double-time is a novel Drosophila clock gene that regulates PERIOD protein accumulation.* Cell, 1998. **94**(1): p. 83-95.

35. Kloss, B., et al., *Phosphorylation of period is influenced by cycling physical associations of double-time, period, and timeless in the Drosophila clock.* Neuron, 2001. **30**(3): p. 699-706.

36. Cyran, S.A., et al., *The double-time protein kinase regulates the subcellular localization of the Drosophila clock protein period.* J Neurosci, 2005. **25**(22): p. 5430-7.

37. Akten, B., et al., *A role for CK2 in the Drosophila circadian oscillator.* Nat Neurosci, 2003. **6**(3): p. 251-7.

38. Lin, J.M., A. Schroeder, and R. Allada, *In vivo circadian function of casein kinase 2 phosphorylation sites in Drosophila PERIOD.* J Neurosci, 2005. **25**(48): p. 11175-83.

39. Smith, E.M., et al., *Dominant-negative CK2alpha induces potent effects on circadian rhythmicity.* PLoS Genet, 2008. **4**(1): p. e12.

40. Harms, E., M.W. Young, and L. Saez, *CK1 and GSK3 in the Drosophila and mammalian circadian clock.* Novartis Found Symp, 2003. **253**: p. 267-77; discussion 102-9, 277-84.

41. Ko, H.W., J. Jiang, and I. Edery, *Role for Slimb in the degradation of Drosophila Period protein phosphorylated by Doubletime.* Nature, 2002. **420**(6916): p. 673-8.

42. Stoleru, D., et al., *The Drosophila circadian network is a seasonal timer.* Cell, 2007. **129**(1): p. 207-19.

43. Blau, J. and M.W. Young, *Cycling vrille expression is required for a functional Drosophila clock.* Cell, 1999. **99**(6): p. 661-71.

44. Cyran, S.A., et al., *vrille, Pdp1, and dClock form a second feedback loop in the Drosophila circadian clock.* Cell, 2003. **112**(3): p. 329-41.

45. Glossop, N.R., et al., *VRILLE feeds back to control circadian transcription of Clock in the Drosophila circadian oscillator.* Neuron, 2003. **37**(2): p. 249-61.

46. Chang, D.C. and S.M. Reppert, *A Novel C-Terminal Domain of Drosophila PERIOD Inhibits dCLOCK:CYCLE-Mediated Transcription.* Curr Biol, 2003. **13**(9): p. 758-762.

47. Zylka, M.J., et al., *Molecular analysis of mammalian timeless.* Neuron, 1998. **21**(5): p. 1115-22.

48. Sato, T.K., et al., *A functional genomics strategy reveals Rora as a component of the mammalian circadian clock.* Neuron, 2004. **43**(4): p. 527-37.

49. Takano, A., Y. Isojima, and K. Nagai, *Identification of mPer1 phosphorylation sites responsible for the nuclear entry.* J Biol Chem, 2004. **279**(31): p. 32578-85.

50. Shirogane, T., et al., *SCFbeta-TRCP controls clock-dependent transcription via casein kinase 1-dependent degradation of the mammalian period-1 (Per1) protein.* J Biol Chem, 2005. **280**(29): p. 26863-72.

51. Iitaka, C., et al., *A role for glycogen synthase kinase-3beta in the mammalian circadian clock.* J Biol Chem, 2005. **280**(33): p. 29397-402.

52. Wang, J., L. Yin, and M.A. Lazar, *The orphan nuclear receptor Rev-erb alpha regulates circadian expression of plasminogen activator inhibitor type 1*. J Biol Chem, 2006. **281**(45): p. 33842-8.

53. Wijnen, H. and M.W. Young, *Interplay of circadian clocks and metabolic rhythms.* Annu Rev Genet, 2006. **40**: p. 409-48.

54. Fu L, et al., *The circadian gene Period2 plays an important role in tumor suppression and DNA damage response in vivo.* Cell, 2002. **111**: p. 441-50.

55. Rosbash, M. and J.S. Takahashi, *Circadian rhythms: the cancer connection.* Nature, 2002. **420**(6914): p. 373-4.

56. Desan, P.H., et al., *Genetic polymorphism at the CLOCK gene locus and major depression.* Am J Med Genet, 2000. **96**(3): p. 418-21.

57. Johansson, C., et al., *Circadian clock-related polymorphisms in seasonal affective disorder and their relevance to diurnal preference.* Neuropsychopharmacology, 2003. **28**(4): p. 734-9.

58. Lamont, E.W., et al., *The role of circadian clock genes in mental disorders.* Dialogues Clin Neurosci, 2007. **9**(3): p. 333-42.

59. So, W.V. and M. Rosbash, *Post-transcriptional regulation contributes to Drosophila clock gene mRNA cycling.* EMBO J, 1997. **16**(23): p. 7146-55.

60. Bao, S., et al., *The Drosophila double-timeS mutation delays the nuclear accumulation of period protein and affects the feedback regulation of period mRNA.* J Neurosci, 2001. **21**(18): p. 7117-26.

61. Martinek, S., et al., *A role for the segment polarity gene shaggy/GSK-3 in the Drosophila circadian clock.* Cell, 2001. **105**(6): p. 769-79.

62. Sakakida, Y., et al., *Importin alpha/beta mediates nuclear transport of a mammalian circadian clock component, mCRY2, together with mPER2, through a bipartite nuclear localization signal.* J Biol Chem, 2005. **280**(14): p. 13272-8.

63. Saez, L. 2008.

64. Chang, D.C. and S.M. Reppert, *A novel C-terminal domain of drosophila PERIOD inhibits dCLOCK:CYCLE-mediated transcription.* Curr Biol, 2003. **13**(9): p. 758-62.

65. Nawathean, P., D. Stoleru, and M. Rosbash, *A small conserved domain of Drosophila PERIOD is important for circadian phosphorylation, nuclear localization, and transcriptional repressor activity.* Mol Cell Biol, 2007. **27**(13): p. 5002-13.

66. Dardente, H., et al., *Cryptochromes impair phosphorylation of transcriptional activators in the clock: a general mechanism for circadian repression.* Biochem J, 2007. **402**(3): p. 525-36.

67. He, Q., et al., *CKI and CKII mediate the FREQUENCY-dependent phosphorylation of the WHITE COLLAR complex to close the Neurospora circadian negative feedback loop.* Genes Dev, 2006. **20**(18): p. 2552-65.

68. Morais Cabral, J.H., et al., *Crystal structure and functional analysis of the HERG potassium channel N terminus: a eukaryotic PAS domain.* Cell, 1998. **95**(5): p. 649-55.

69. Gu, Y.Z., J.B. Hogenesch, and C.A. Bradfield, *The PAS superfamily: sensors of environmental and developmental signals.* Annu Rev Pharmacol Toxicol, 2000. **40**: p. 519-61.

70. Taylor, B.L. and I.B. Zhulin, *PAS domains: internal sensors of oxygen, redox potential, and light.* Microbiol Mol Biol Rev, 1999. **63**(2): p. 479-506.

71. Pellequer, J.L., et al., *Photoactive yellow protein: a structural prototype for the three-dimensional fold of the PAS domain superfamily.* Proc Natl Acad Sci U S A, 1998. **95**(11): p. 5884-90.

72. Genick, U.K., et al., *Structure at 0.85 A resolution of an early protein photocycle intermediate.* Nature, 1998. **392**(6672): p. 206-9.

73. Perutz, M.F., M. Paoli, and A.M. Lesk, *Fix L, a haemoglobin that acts as an oxygen sensor: signalling mechanism and structural basis of its homology with PAS domains.* Chem Biol, 1999. **6**(11): p. R291-7.

74. Gong, W., et al., *Structure of a biological oxygen sensor: a new mechanism for heme-driven signal transduction.* Proc Natl Acad Sci U S A, 1998. **95**(26): p. 15177-82.

75. Crosson, S. and K. Moffat, *Structure of a flavin-binding plant photoreceptor domain: insights into light-mediated signal transduction.* Proc Natl Acad Sci U S A, 2001. **98**(6): p. 2995-3000.

76. Vreede, J., et al., *PAS domains. Common structure and common flexibility.* J Biol Chem, 2003. **278**(20): p. 18434-9.

77. Dioum, E.M., et al., *NPAS2: a gas-responsive transcription factor.* Science, 2002. **298**(5602): p. 2385-7.

78. Kaasik, K. and C.C. Lee, *Reciprocal regulation of haem biosynthesis and the circadian clock in mammals.* Nature, 2004. **430**(6998): p. 467-71.

79. Zheng, B., et al., *The mPer2 gene encodes a functional component of the mammalian circadian clock.* Nature, 1999. **400**(6740): p. 169-73.

80. Yagita, K., et al., *Dimerization and nuclear entry of mPER proteins in mammalian cells.* Genes Dev, 2000. **14**(11): p. 1353-63.

81. Vielhaber, E., et al., *Nuclear entry of the circadian regulator mPER1 is controlled by mammalian casein kinase I epsilon.* Mol Cell Biol, 2000. **20**(13): p. 4888-99.

82. Millar, A.J., *Circadian rhythms: PASsing time.* Curr Biol, 1997. **7**(8): p. R474-6.

83. Saez, L. and M.W. Young, *Regulation of nuclear entry of the Drosophila clock proteins period and timeless.* Neuron, 1996. **17**(5): p. 911-20.

84. Gekakis, N., et al., *Isolation of timeless by PER protein interaction: defective interaction between timeless protein and long-period mutant PERL.* Science, 1995. **270**(5237): p. 811-5.

85. Baylies, M.K., et al., *New short period mutations of the Drosophila clock gene per.* Neuron, 1992. **9**(3): p. 575-81.

86. Huang, Z.J., K.D. Curtin, and M. Rosbash, *PER protein interactions and temperature compensation of a circadian clock in Drosophila.* Science, 1995. **267**(5201): p. 1169-72.

87. Zeng, H., et al., *A light-entrainment mechanism for the Drosophila circadian clock.* Nature, 1996. **380**(6570): p. 129-35.

88. Schotland, P., et al., *Altered entrainment and feedback loop function effected by a mutant period protein.* J Neurosci, 2000. **20**(3): p. 958-68.